**Environmental Science-nano**
May 2019, Volume 6 Issue 5 Pages 1363-1381
https://doi.org/10.1039/c8en00987b
https://archimer.ifremer.fr/doc/00792/90391/



# Transcriptomic response of the benthic freshwater diatom *Nitzschia palea* exposed to Few Layer Graphene

Garacci Marion [1], Barret Maialen [1, *], Folgoas Clement [2], Flahaut Emmanuel [3], Chimowa George [3], Bertucci Anthony [4], Gonzalez Patrice [4], Silvestre Jerome [1], Gauthier Laury [1], Zouine Mohamed [2], Pinelli Eric [1]

[1] EcoLab, Université de Toulouse, CNRS, Toulouse, France.
[2] GBF (Laboratoire Génomique et Biotechnologie du Fruit), ENSAT, INRA/INP, UMR 990, Castanet Tolosan, France
[3] Institut Carnot CIRIMAT (Centre Inter-universitaire de Recherche et d'Ingénierie des MATériaux), Université de Toulouse, INP, UPS, UMR CNRS 5085, Toulouse, France
[4] Université de Bordeaux, UMR EPOC CNRS 5805, Pessac, France

* Corresponding author : Maialen Barret, email address : maialen.barret@ensat.fr

**Abstract :**

Nanotechnology is currently undergoing rapid development partly due to the increasing use of carbon-based nanoparticles, such as Few Layer Graphene (FLG). Owing to its numerous applications, its industrial production is likely to lead to environmental release, including into aquatic ecosystems. In this study, a transcriptomic approach was used to assess the effect of FLG at low (0.1 mg L-1) and high (50 mg L-1) concentrations on the benthic freshwater diatom Nitzschia palea after 48 h of exposure. Direct contact with FLG and induced shading were distinguished to compare the transcriptomic responses. Genes that were differentially expressed after exposure compared with control conditions were identified, and their functional descriptions are discussed. A slight transcriptomic response related to cell wall repair was observed in diatoms exposed to the low FLG concentration. Exposure to the high FLG concentration induced a strong response involving 1907 transcripts. Notably, 16 transcripts involved in the chlorophyll biosynthesis process were under-expressed (log2 fold change between -3 and -1.2), suggesting a down-regulation of the photosynthetic metabolism. Diatoms exposed to the high FLG concentration over-expressed about 13 transcripts encoding for extracellular proteins that play a role in cellular adhesion, and two transcripts involved in cell wall repair were highly up-regulated. Light deprivation caused by shading induced a downregulation of genes involved in the energetic metabolism of N. palea. Overall, these results revealed that metabolic pathways impacted by FLG exposure are concentration and contact dependent. Moreover, this study suggests that a low FLG concentration, close to that in environmental conditions, will have a minor impact on diatom biofilms whereas a high FLG concentration, mimicking accidental release, might be critical for ecosystems.

## Graphical abstract

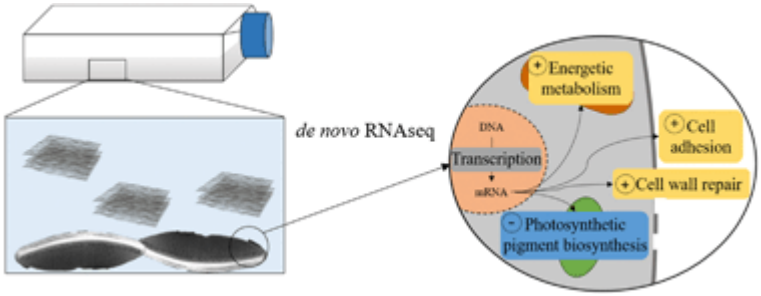

## 1. Introduction

The use of nanoparticles in everyday-life items available on the market place is now established[1]. Nowadays, industrials seek to optimize performance and quality of products already commercialized, thanks to the use of nanomaterials. Notably, the development of nanocomposite-based products allows for miniaturizing technologies. Nanotechnology has been a fast-growing science in the last few years. The number of nanomaterials-based products was multiplied by thirty in less than a decade [2,3]. The scientists' interest for carbon nanoparticles such as graphene and its derivatives is particularly rising because of their specific properties[4]. The graphene nanomaterials' family encompasses graphene, strictly speaking (composed of a monoatomic carbon layer), and related materials including Few Layer Graphene (FLG). The particular properties of FLG are provided by the nanometric thickness of its planar carbon-based sheets. Several monoatomic layers composed of $sp^2$-bonded carbon atoms in a honeycomb lattice (graphene) are overlapped to form FLG. The thickness in the nanometric range confers industrially interesting properties such as lightness, bendability, and exceptional electrical and thermal conductivity[5–8]. All these properties move FLG from research laboratory to the market driven by demand from industries ranging from energy to biomedicine[9–11]. The use of these nanomaterials offers attractive economical perspectives in several industrial fields[12].

Yet, no strict regulation is yet established for nanomaterials production [13]. Information about real quantities of carbon-based nanoparticles in circulation are not available, especially in the case of graphene. Thus, unknown nanoparticles' amounts may be discharged in waste water from industry and individual households, and then finally released in the environment. Aquatic ecosystems are the final receptacle of pollution through different hydro-geochemical processes, such as atmospheric deposition, lixiviation and leaching of soils. In aquatic ecosystems, nanoparticles might interact with biological systems and cause disturbances. Their theoretically exceptionally high specific area and the difficulty to predict the release and fate in the aquatic ecosystems make FLG a worrying emerging contaminant[14–16]. In spite of this, the evaluation of the environmental risk of FLG is still in its infancy and a strong lack of information persists regarding its potential impact on aquatic ecosystems[17].

Diatoms constitute a particular branch of unicellular microalgae with the ability to produce a cell wall, called frustule, composed of silica with different ornamentations depending on species. Diatoms are known to play a major role in the global primary productivity of the

aquatic ecosystem[18,19]. They represent the main cellular component of freshwater biofilm when environmental conditions are not optimal for green algae. Some diatom species are able to resist to organic pollution and the diatom community composition can be used as a bioindicator of the ecological state of freshwater[20]. Within biofilm, diatoms and other organisms are able to produce extracellular polymeric substances (EPS) mainly composed of polysaccharides and proteins[21]. Several roles are proposed to the excretion of EPS, but the primary and major role of this external matrix is to help diatoms to adhere and grow on a substrate. Secondly, the EPS matrix was found to procure a protection against pollutants such as metals[22] or carbon nanoparticles such as carbon nanotubes[23] or FLG[24]. Pollutants are then accumulated in the extracellular matrix and removed from the water column. However, the biochemical structure of substances responsible for the trapping of nanoparticles is still to be elucidated.

Environmental nanotoxicity studies assessing the effects of FLG are scarce. Most of the studies considering the impact of graphene family material focused on the graphene oxide, which carries (among others) epoxide functions on the surface of the carbon layer. Inhibition of root development followed by an adaptation of terrestrials plants exposed to 0.01 to 1 $mg.L^{-1}$ was demonstrated[25,26].. An interesting work carried out on zebrafish larvae exposed to 25 to 100 $mg.L^{-1}$ graphene quantum dots (GQD; crystalline nanostructure smaller than a nanoparticle with high photoluminescence properties) revealed an acute inflammatory response linked to an activation of the detoxifying system[27]. Graphene nanoplatelets (GNP) toxicity on *Pseudomonas aeruginosa* was evaluated by Mortimer and his co-workers (2018)[28]. The authors suggested that GNP (10 $mg.L^{-1}$) had no antibacterial activity, but could affect bacterial physiology and metabolism.

Potential accumulation in the sediment and subsequent transfer of nanoparticles along the food chain through biomagnification justifies the relevance of ecotoxicological studies towards microbial organisms which are essential to the biogeochemical cycles of aquatic ecosystems. Despite the crucial role of photosynthetic organisms in the ecosystem functioning, only few studies evaluated the effect of graphene family nanoparticles on algae. Hu and co-workers (2014)[29] reported an internalisation of graphene oxide nanoparticles in *Chlorella vulgaris* cells, leading to the alteration of chloroplast structure and the increase in Reactive Oxygen Species (ROS) production. Few years later, the same authors demonstrated the contribution of the fatty acid metabolism to ROS levels, adding that cell plasmolysis was associated with a carbohydrate consumption[30].

To evaluate the nanotoxicity on aquatic organisms, transcriptomics, proteomics and metabolomics are up-to-date powerful tools[31,32]. Indeed, they provide an accurate, high-throughput and hypothesis-independent description of the mechanisms involved in stress response. Omic approaches enables to establish the relationship between molecular endpoints and global metabolic response at low contaminants concentration and on all kind of organisms[33,34]. Transcriptomic and proteomic studies conducted on diatoms are limited[35–38], and have hardly ever been applied to nanotoxicology. Transcriptomic approach was used to study the effect of zinc oxide nanoparticles on a marine diatoms[39], but to the author's knowledge, no study was performed on the impact of carbon nanoparticles on freshwater diatoms.

Cellular responses of *N. palea* (Kützing) W. Smith (*N. palea*) exposed to FLG (0.1, 1, 10 and 50 $mg.L^{-1}$) were assessed in a previous work studying the impact on cellular growth and photosynthesis activity[24]. Based on these endpoints, diatom response to FLG was detected only at 50 $mg.L^{-1}$. Moreover, the sticking of FLG nanoparticles in diatoms biofilm was appreciated thanks to a monitoring of FLG fate in the water column and in the biofilm. The current study aims at assessing the molecular response of this diatom exposed to FLG using a transcriptomic analysis. Here, we analysed the difference of the transcriptomic response of diatoms exposed to growth inhibitory and non-inhibitory FLG concentrations. We tested two doses of FLG: one dose, close to a potential environmental concentration (0.1 $mg.L^{-1}$) and a high one (50 $mg.L^{-1}$), which could correspond to an accidental release of nanoparticles. We also distinguished the shading part of the total impact of FLG exposure at high concentration.

## 2. Materials and methods

### 2.1. Preparation of graphene suspension

The synthesis of FLG was carried out by an exfoliation process from expandable graphite flakes provided by Asbury Carbons (Ref. 3772). Expandable graphite was prepared by industrial intercalation of acids in order to facilitate the exfoliation process. A thermal expansion was performed from 12.95 g of expandable graphite flakes divided in batches. Details of the synthesis method to obtain FLG is described in Appendix 1. The final equivalent weight of dry FLG was 530 mg which corresponded to a yield of 4.1 wt. % from the starting expandable graphite.

The wet FLG was diluted in SPE medium sterilized 20min at 121°C and bath sonicated for 10 min (Elmasonic S30H, 280W). Immediately after a second short bath sonication of 2 min of

the FLG suspension, dilutions were carried out under axenic conditions before the experiments in order to avoid contamination. Homogenous intermediary FLG suspension were then prepared at 0.167 and 83.5 $mg.L^{-1}$ to reach a final concentration in the experimental device of 0.1 ($FLG_{0.1}$) and 50 $mg.L^{-1}$ ($FLG_{50}$) respectively. Just before the addition of FLG to the diatoms culture, a last sonication was performed to ensure a good dispersion of nanoparticles in the exposure medium.

### 2.2. FLG characterization

A small quantity of FLG suspension was frozen and freeze-dried (Christ Alpha 2-4 LSC) in order to perform a Transmission Electronic Microscopy (TEM, JEOL JEM 1400) observation to determine their size and morphology. Sample was dispersed by bath sonication in ethanol for 10 min and then deposited on a TEM grid (Lacey carbon). Raman spectroscopy analysis on a Labram-HR800 (Horiba) was performed using a laser at 633 nm in confocal mode (x100 magnification, 100 µm hole, diaphragm D1, 20 s exposition, 10 accumulations). Chemical analysis of the samples was obtained by XPS (Kα ThermoScientific, monochromatic Al-Kα source).

### 2.3. Diatoms culture and exposure

#### 2.3.1. Diatoms pre-cultivation

Axenic *N. palea* CPCC-160 strain was purchased from the Canadian Phycological Culture Centre (University of Waterloo, Waterloo, ON, Canada). To maintain axenic conditions of this strain, diatoms were handled under a class II laminar flow hood to avoid biotic contamination. The culture medium used was a sterilized modified CHU N° 10 basic medium, called SPE medium (SPE; 6.4< pH< 6.6). The amplification of the algal culture and the experiments were carried out in a growth room at 22 ± 1 °C on a rotary shaker at 50 rpm with a light/dark period of 14 h/10 h supplied by led Floodlight 150W Dimmable (Vegeled, Colasse SA, Belgium) at 60±10 µE. To carry out ecotoxicological tests on diatoms in active phase, the SPE medium was replaced by fresh medium 72 h before each experiment.

#### 2.3.2. Exposure conditions

The principle of the experimental device used was the same than the one developed earlier by Verneuil *et al*. (2014) and described in a previous study[24] where the shading effect of carbon nanoparticles could be distinguished from the overall exposure effect (combined direct exposure and shading). Experiments were performed in 750 mL culture flasks (FALCON®

Cell Culture Flask, 175cm² straight neck vented cap) superposed on each other. These culture flasks were then placed in customised open-top opaque boxes by batches of 18 where the light perception was only provided by the top face of the flasks.

Before the beginning of the exposure to FLG, 15 lower flasks of each system were inoculated with 100 mL of algal culture ($2.5x10^5$ cells.$mL^{-1}$) to establish the algal biofilm. After 48h, 150 mL of dispersed FLG suspension diluted to the appropriate concentration was added to the algal culture to obtain a final volume of 250 mL for each flask corresponding to the condition of total exposure to nanoparticles. In this way, the final FLG concentration were 0.1 and 50 mg.$L^{-1}$. For the shading exposition, only the highest FLG concentration was tested, which was the only one inducing shading effect on diatoms culture[24]. To test the shading impact on the molecular response of diatoms, 150 mL of FLG at a concentration of 83.5 mg.$L^{-1}$ were placed only in the top flask of the experimental system. All of the flasks which did not contain a final volume of 250 mL were filled with SPE medium (250 mL in the superior flask of the total exposure condition, 150 mL in the lower flask and 100 mL in the upper one of the shading exposure condition). Flasks were placed in a growth room for 48h. Each experimental condition was conducted in triplicate.

### 2.4. RNA extraction and *de novo* sequencing

After 48h of incubation, the flasks were collected and all the supernatant was gently removed without resuspending the algal biofilm. Then the biofilm was scrapped into 50 mL of fresh medium, transferred in a 50 mL Falcon tube and centrifuge at 10 000 rpm for 10s. The supernatant was not completely removed and the pellet containing diatoms was transferred in a new 2 mL Eppendorf tube for a final centrifugation to pellet the cells. Once the supernatant removed, the pellets were immediately frozen in liquid nitrogen and store at -80°C until RNA extraction.

Extraction of total RNA was carried out using a modified QIAGEN® kit protocol (RNeasy Plant Mini Kit, 74904, QIAGEN). A first step of cellular lysis was performed using 450µL of TRIzol® Reagent (Invitrogen) combined to grinding with silica beads (Sartorius™ BBI-8541400) (200µL) using a FastPrep® (FastPrep®-24 Classic Instrument, MP Biomedicals, 6.5 m.$s^{-1}$, 6x20s). Samples were then heated at 56°C for 10min to separate RNA from carbon-based nanoparticles, since these nanoparticles are known to strongly interact with nucleic acids through adsorption onto nanoparticles surfaces[41]. A first extraction step with 200µL of chloroform RECTAPUR (VWR) was followed by the RNA isolation and purification on

QIAGEN® RNeasy Mini Spin column to bind total RNA. Potential small quantity of DNA in the sample was suppressed thanks to a 15min DNAse I treatment at room temperature. The final elution was carried out in 40µL of RNase free water. The yield and quality of RNA samples were assessed using a Nanodrop spectrophotometer. RNA concentration ranged from 99 to 3,091.5 ng.µL$^{-1}$ . The ratio of absorbance at 260 and 280 nm was higher than 2. RNA integrity was checked by a microgel electrophoresis on an Experion™ Electrophoresis Automated System using a Experion™ RNA StdSens Analysis kit. RIN ranged from 5 to 7.5. Samples were stored at -80°C prior to sequencing. RNA samples were sent to GATC Biotech SARL platform for RNA sequencing. A next generation Illumina paired end sequencing was performed on each replicate with a strand specific cDNA library generated and insert size of 150pb resulting in about 30 million reads (± 3%). This Transcriptome Shotgun Assembly project has been deposited at DDBJ/ENA/GenBank under the accession GHBX00000000 in the BioProject named "Nitzschia palea Transcriptome" (Accession number: PRJNA489196). The version described in this paper is the first version, GHBX01000000. Due to the low number of related and annotated diatoms sequences in databases, the interpretation of the results must be taken with care.

### 2.5. RNA-seq *de novo* assembly and quantification analysis

Reads assembly was performed using the De novo RNA-seq Assembly Pipeline (DRAP)[42] including the trimming of low quality bases. A transcriptome was generated for each conditions and a metatranscriptome was obtained. Reads were mapped on this assembled metatranscriptome using the Trinity Transcripts Quantification v2.4.0[43] applying the RNA-Seq by Expectation-Maximization method[44]. Annotation and Gene Ontology (GO) mapping of the *N. palea* metatranscriptome were carried out with the Blast2GO software using default parameters [45]. Transcripts were compared to the non-redundant 'nr' database using the BLASTx tool with a similarity and annotation parameter threshold (e-value) of 1.10$^{-3}$ (probability with which an alignment with greater similarity is expected to be found by chance). Differential expression analysis was inferred based on the normalized counts with the statistical open source software R[46] using the "DESeq2" package[47]. For all the differentially expressed genes (DEGs) with a p-value < 0.05, a GO Enrichment analysis was performed using the "topGO" R package[48]. The "topGO" outcomes were implemented in the open web-based tool QuickGO[49] to generate GO trees for each condition and each GO category (Biological Process, Molecular Function and Cellular Component). All the enriched GO terms for these DEGs were aggregated at the same GO level in order to simplify the

comparison of Biological Process involved between conditions. R packages "gplots"[50] and "RColorBrewer"[51] were used to generate heat maps of gene expression, and "VennDiagram" package[52] to represent the numbers of DEGs shared between conditions.

## 3. Results and Discussion

### 3.1. Characterization of FLG

The initial expandable graphite and the method used to produce FLG suspension were exactly the same as the ones used in a previous study[24]. The full description of FLG nanoparticles is thus provided in this previous study. Briefly, FLG nanoparticles present a number of layers estimated between 5 and 10 with an interlayer distance of 0.34 nm. Figure 1 shows TEM

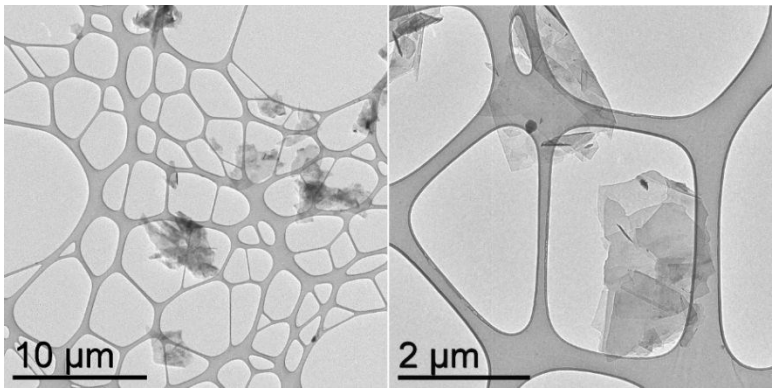


***Figure 1.*** *Transmission Electronic Microscopy of dried FLG.*

observations of FLG nanoparticles.

To avoid misinterpretations due to the presence of other pollutants in the FLG suspensions[53] which could be linked to the mode of production, ICP-OES analyses were also performed on previous FLG sample revealing the absence of release of metallic ions or absorption of nutrients by FLG in the culture medium.

### 3.2. Assembly and annotation statistics

Next Generation Sequencing and RNA-seq assembly generated an unprecedented *N. palea* transcriptome. A total of 15,906 transcripts ranging from 230 to 24,434 bp (N50 = 2,139 bp) were obtained after running the DRAP pipeline. The generated *N. palea* transcriptome presented an estimated recovery of 69-97% of its sequenced genome (not published yet). The obtained *N. palea* transcriptome thus ensures a consistent analysis based on reads quantification. Functional annotation of *N. palea* transcriptome revealed that 17.5% of the transcripts did not match with referenced sequences in the database we used. Indeed, 15 to

50% of the ten most up- and down-expressed transcripts (Log2FoldChange: Log2FC) could not be associated with a GO term (Table 1) in the conditions tested.

This non-negligible percentage revealed the lack of information for this species. Nevertheless, the percentage of annotation was relatively similar for Hook and co-workers (2014)[36] with the marine diatom *Ceratoneis closterium* transcriptome that contained 36.3% of non-annotated transcripts. In other transcriptomic studies on diatoms, this percentage was not reached, with 33% of annotation for *Thalassiosira pseudonana*[37] or 27.6% for the diatom *Leptocylindrus aporus*[38]. Only few transcriptomic or genomic studies have been performed on diatoms, mainly on marine species, leading to a persistent paucity of sequence information available[36]. Indeed, the genome sequence of only four marine diatoms are currently available: *T. pseudonana* [54] and *Phaeodactylum tricornutum*[55], *T. oceanica*[56], *Fragilariopsis cylindricus*[57].

***Table 1***. *Characteristics of the 'top ten' up and down-regulated differentially expressed transcripts (compared to the control condition) in each exposure condition: $FLG_{0.1}$ (FLG0.1), $FLG_{50}$ (FLG50) and shading $FLG_{50}$ (Shading FLG50). The ten most upregulated transcripts are listed in the first part of this table and the ten most downregulated transcripts in the second part. Grey numbers indicate the standard error for the Log2FC values. The column* Description *corresponds to the output of the transcript annotation on Blast2GO.*

| Transcript ID | Description | Log2FC | P-value | Number of GO term |
|---|---|---|---|---|
| FLG0.1 – Up-regulated | | | | |
| TC01_diatome_k31_Locus_1015_Transcript_19_7 | ---NA--- | 3.98 0.87 | 5.42E-03 | 0 |
| TG01_diatome_k49_Locus_8806_Transcript_3_1 | predicted protein | 3.36 0.74 | 5.74E-03 | 8 |
| OG50_diatome_k49_Locus_3306_Transcript_2_1 | peptide methionine sulfoxide reductase | 3.14 0.80 | 3.64E-02 | 2 |
| TT00_diatome_k25_Locus_10139_Transcript_2_1 | hypothetical protein FRACYDRAFT_240855 | 2.90 0.42 | 1.10E-07 | 0 |
| TC01_diatome_k25_Locus_143_Transcript_9_3 | ---NA--- | 2.82 0.63 | 7.87E-03 | 0 |
| TG01_diatome_k31_Locus_216_Transcript_1_2 | phosphatidylinositol-3-phosphatase myotubularin-2-like | 2.79 0.48 | 5.30E-05 | 0 |
| OG50_diatome_CL18Contig1_1 | carbohydrate-binding module family 18 | 2.66 0.65 | 2.64E-02 | 2 |
| TG01_diatome_k37_Locus_3478_Transcript_1_1 | predicted protein | 2.64 0.56 | 3.59E-03 | 2 |
| OG50_diatome_k31_Locus_629_Transcript_1_1 | ---NA--- | 2.56 0.50 | 9.68E-04 | 0 |
| TC01_diatome_k49_Locus_13493_Transcript_1_1 | ---NA--- | 2.55 0.59 | 1.35E-02 | 0 |
| FLG50 – Up-regulated | | | | |
| TC01_diatome_CL15Contig1_1 | ---NA--- | 6.97 1.41 | 5.86E-05 | 0 |
| TT00_diatome_CL78Contig1_1 | extracellular matrix | 5.82 1.30 | 3.86E-04 | 8 |
| TG01_diatome_k37_Locus_8797_Transcript_1_1 | Bv80 Bb- | 5.80 1.36 | 8.12E-04 | 2 |
| TG01_diatome_k49_Locus_6869_Transcript_1_1 | vegetative cell wall gp1-like | 5.72 0.84 | 5.33E-09 | 2 |
| OG50_diatome_k31_Locus_8965_Transcript_2_1 | ---NA--- | 5.59 1.05 | 1.01E-05 | 0 |
| OG50_diatome_k49_Locus_10629_Transcript_1_1 | zinc finger | 5.26 0.62 | 1.16E-13 | 0 |
| OG50_diatome_CL11Contig3_2 | filamentous hemagglutinin family N-terminal domain | 5.06 0.79 | 6.88E-08 | 5 |
| TC01_diatome_k49_Locus_10503_Transcript_2_1 | ubiquitin thioesteraseVirion core | 5.06 1.35 | 4.31E-03 | 1 |
| TG01_diatome_k37_Locus_4954_Transcript_4_1 | SPT2 homolog | 4.96 0.72 | 3.97E-09 | 6 |
| OG50_diatome_k43_Locus_9941_Transcript_1_1 | non-classical arabinogalactan 31 | 4.80 0.82 | 1.11E-06 | 0 |
| Shading FLG50 – Up-regulated | | | | |
| TG01_diatome_CL991Contig1_2 | ---NA--- | 1.94 0.48 | 3.65E-02 | 0 |
| TC01_diatome_k31_Locus_1657_Transcript_18_1 | cell surface receptor | 1.38 0.29 | 3.64E-03 | 3 |
| TG01_diatome_CL343Contig1_1 | PIN2 TERF1-interacting telomerase inhibitor 1 | 1.04 0.23 | 9.88E-03 | 1 |

| Transcript ID | Description | Log2FC | | P-value | Number of GO term |
|---|---|---|---|---|---|
| FLG0.1 – Down-regulated | | | | | |
| TG01_diatome_k25_Locus_7929_Transcript_2_2 | digalactosyldiacylglycerol synthase chloroplastic-like | -1.09 | 0.26 | 1.59E-02 | 3 |
| TG01_diatome_k31_Locus_6207_Transcript_8_1 | Spindle assembly abnormal 6-like | -1.17 | 0.30 | 3.35E-02 | 0 |
| TT00_diatome_k31_Locus_117_Transcript_12_2 | P-loop containing nucleoside triphosphate hydrolase | -1.46 | 0.35 | 1.76E-02 | 1 |
| OG50_diatome_k25_Locus_808_Transcript_10_4 | P-loop containing nucleoside triphosphate hydrolase | -1.53 | 0.36 | 1.78E-02 | 1 |
| TC01_diatome_k37_Locus_8958_Transcript_1_1 | Leucine-rich repeat-containing | -1.58 | 0.37 | 1.29E-02 | 0 |
| TC01_diatome_k25_Locus_1280_Transcript_8_1 | P-loop containing nucleoside triphosphate hydrolase | -1.67 | 0.42 | 2.88E-02 | 1 |
| FLG50 – Down-regulated | | | | | |
| TG01_diatome_k49_Locus_3860_Transcript_5_3 | Light harvesting complex | -3.01 | 0.65 | 1.92E-04 | 5 |
| OG50_diatome_k49_Locus_999_Transcript_1_1 | peptidyl-prolyl cis-trans isomerase | -3.13 | 1.03 | 2.57E-02 | 3 |
| TT00_diatome_k25_Locus_2148_Transcript_2_3 | hypothetical protein THAOC_23078 | -3.17 | 0.85 | 4.26E-03 | 0 |
| TG01_diatome_k37_Locus_3478_Transcript_1_1 | predicted protein | -3.33 | 0.57 | 1.30E-06 | 2 |
| TT00_diatome_k49_Locus_11252_Transcript_1_1 | hypothetical protein FisN_6Lh195 | -3.52 | 0.89 | 2.40E-03 | 1 |
| TG01_diatome_k25_Locus_2756_Transcript_6_1 | FKBP-type peptidyl-prolyl cis-trans isomerase | -3.60 | 0.77 | 1.96E-04 | 5 |
| TC01_diatome_k31_Locus_10410_Transcript_1_1 | ---NA--- | -4.21 | 1.42 | 3.11E-02 | 0 |
| OG50_diatome_k25_Locus_114_Transcript_2_1 | predicted protein | -4.44 | 1.57 | 4.11E-02 | 3 |
| TT00_diatome_CL2065Contig1_2 | Calcium calmodulin dependent kinase association-domain | -4.67 | 0.99 | 1.43E-04 | 3 |
| OG50_diatome_k49_Locus_3306_Transcript_2_1 | peptide methionine sulfoxide reductase | -4.75 | 0.82 | 1.42E-06 | 2 |
| Shading FLG50 – Down-regulated | | | | | |
| OG50_diatome_k43_Locus_3019_Transcript_2_1 | fatty acid oxidation alpha mitochondrial | -1.88 | 0.43 | 1.02E-02 | 4 |
| TC01_diatome_CL1592Contig1_1 | enoyl- hydratase | -1.97 | 0.39 | 1.44E-03 | 1 |
| TT00_diatome_k37_Locus_2515_Transcript_3_1 | phosphoenolpyruvate carboxykinase (ATP) | -2.07 | 0.44 | 3.64E-03 | 6 |
| TT00_diatome_k31_Locus_4388_Transcript_4_1 | 3-ketoacyl- mitochondrial | -2.14 | 0.54 | 4.00E-02 | 3 |
| TG01_diatome_k31_Locus_5498_Transcript_4_1 | ubiquitin-superoxide dismutase fusion | -2.18 | 0.56 | 4.78E-02 | 4 |
| TC01_diatome_CL336Contig1_1 | glyceraldehyde-3-phosphate dehydrogenase | -2.23 | 0.56 | 4.00E-02 | 7 |
| TT00_diatome_k37_Locus_4335_Transcript_2_1 | 3-ketoacyl- mitochondrial | -2.33 | 0.52 | 8.73E-03 | 4 |
| TT00_diatome_k25_Locus_1348_Transcript_2_1 | aldehyde dehydrogenase | -2.75 | 0.44 | 3.60E-06 | 8 |
| TC01_diatome_k31_Locus_1897_Transcript_2_2 | phosphoenolpyruvate carboxykinase | -2.88 | 0.49 | 1.75E-05 | 1 |
| TC01_diatome_k37_Locus_4112_Transcript_2_3 | ---NA--- | -3.07 | 0.55 | 8.61E-05 | 0 |

***Table 1***. *Continued*

### 3.3. Differential expression

The differential expression analysis was performed to identify DEGs after 48h under each exposure condition. Among the 15,906 transcripts, 1,953 DEGs (12.3 %) were differentially expressed. No selection on Log2FC values was applied on these DEGs in order to conserve the slightest up- or downregulated DEGs. This percentage of DEGs was higher than that found in previous studies carried out on the marine diatoms *T. pseudonana*, and *C. closterium*, in which DEGs with a Log2FC ≥ 1 or ≥ 3.3, accounted respectively for 6 and 2.5%[36,37]. In these studies, *T. pseudonana* was exposed to an ammonia concentration (4 $mg.L^{-1}$) corresponding to 10% growth inhibition ($IC_{10}$), and *C. closterium* to $IC_{40}$ of the polycyclic aromatic hydrocarbon benzo-a-pyrene (36.45 $\mu g.L^{-1}$). These concentrations were sufficiently high to impact the cellular growth rate but induced a slighter transcriptomic response than obtained in our study. This comparison highlight that conditions tested in our experiments, especially for $FLG_{50}$ exposure, represent considerable conditions inducing strong transcriptomic response. In our DEGs dataset the expression level varied between -4.7 and -0.6 for the down regulated and between 0.5 and 7 for the up-regulated DEGs. This transcript differential expression levels were comparable to that observed by Carvalho, Bopp, and Lettieri (2011)[37] in which the Log2FC reached 7.2. Others studies on diatoms revealed a maximum expression level of 4.9 for a reverse transcriptomic study on *N. palea* exposed to 1 $\mu g.L^{-1}$ diuron[58], and 2.8 in a work on *Leptocylindrus danicus* sexual reproduction[38].

Exposure to the highest FLG concentration was associated with a high number of DEGs, compared to the low FLG concentration and shading condition (Figure 2a). Most of these DEGs were up-regulated in diatoms exposed to 0.1 and 50 $mg.L^{-1}$ of FLG, while down-regulated transcripts represented most of the DEGs in the shading condition. Overall, a consequent proportion of DEGs could not be associated with GO terms, where DEGs involved in diatoms exposed to $FLG_{0.1}$ presented the lowest functional annotation followed by diatoms directly exposed to $FLG_{50}$ and shading exposure in the end (Figure 2b). The comparison of expression profiles obtained in $FLG_{50}$ with the two others conditions showed that diatoms responses were mainly different, with only 13 DEGs shared with $FLG_{0.1}$ and 14 with shading condition (Figure 2c). None of the DEGs was shared between the shading and $FLG_{0.1}$ exposure. This is consistent with a previous study in which we did not detect any

shading effect on cellular response [24]. Diatoms exposed to high FLG concentration exhibited a stronger and specific transcriptomic response compared to $FLG_{0.1}$ and shading conditions.

Within the amount of shared sequences, the number of transcripts regulated in the same way were also identified. Among the 13 transcripts differentially expressed in diatoms directly exposed to low and high FLG concentration, 9 were up-regulated in both conditions with a Log2FC ranging from 1.23±0.35 to 4.48±1.38. These results showed that responses shared between low and high FLG concentrations were weak. Among the 14 DEGs shared between direct and shading exposition to $FLG_{50}$, only one was regulated in the same way. Shading exposure shared few DEGs with direct exposure for the same FLG concentration where the common DEGs were in majority inversely expressed. Regarding these first results, we could suppose that the response induced by direct exposure to $FLG_{50}$ might not be comparable to the response obtained in the shading condition. These results were in accordance with the shading effect observed in a previous study[24] revealing growth inhibition until the end of the experiment while diatoms directly exposed to $FLG_{50}$ showed a temporary growth inhibition after 48h of exposure with a growth recovery at the end of the experiment thanks to the sticking of nanoparticles in the biofilm matrix.

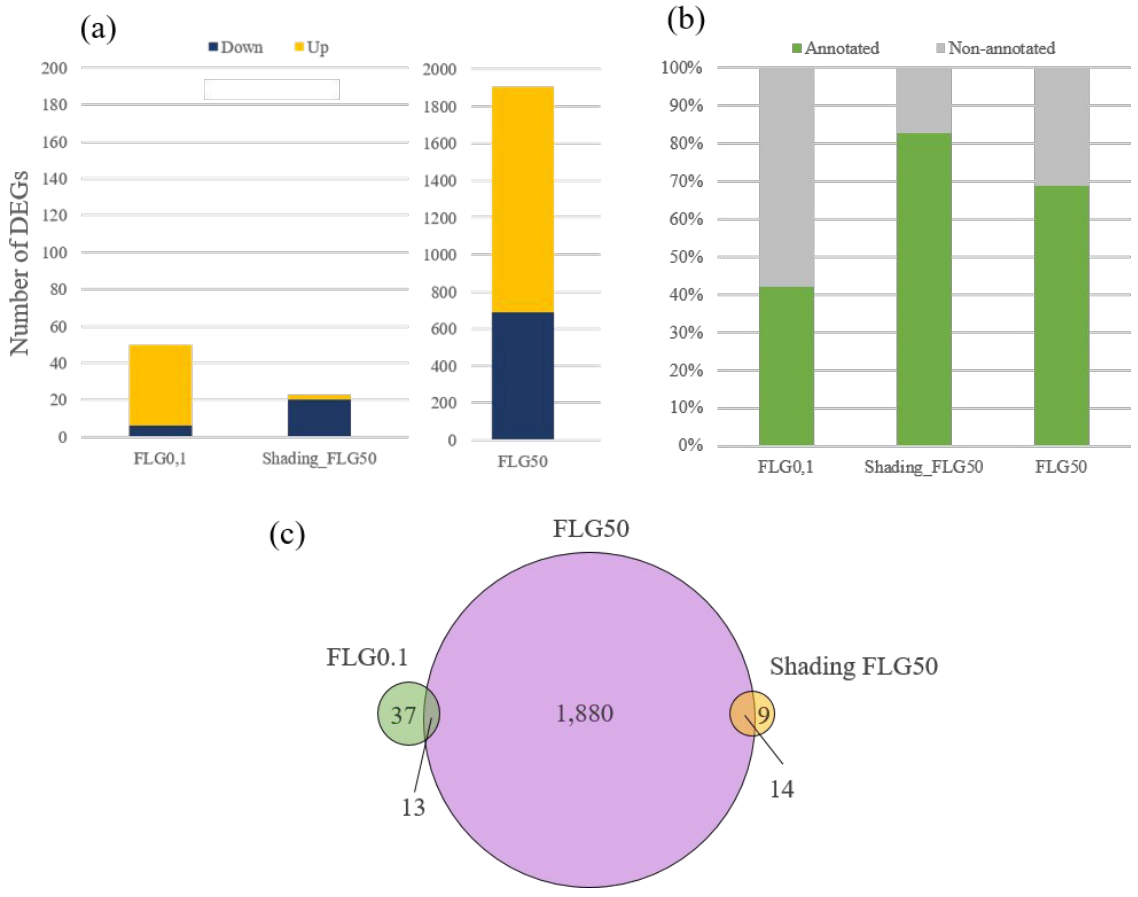


***Figure 2**. Description of the differential expressed genes in the different conditions. (a) Total number of DEGs with the proportion of up and down-regulated transcripts. (b) Percentage of DEGs assigned to a Gene Ontology term. (c) Venn diagram showing the number of shared DEGs between in each exposure condition.*

### 3.4. Functional annotation

Gene ontology annotation and enrichment analysis were performed to identify biological processes, molecular function and cellular components to which DEGs are related. The results shown in this paper primarily concern the Biological Process category, with an overview of Cellular Component category, especially in $FLG_{50}$ condition. Only 3 GO terms were overrepresented for 2 DEGs expressed in $FLG_{0.1}$ condition, 162 GO terms for 599 DEGs in $FLG_{50}$ and 37 GO terms for 8 DEGs in the shading condition. It should be noted that each DEG can be associated with several biological processes and hence carrying multiple GO terms.

Study of the Biological Process involved in diatom's responses to FLG was performed on DEGs with enriched GO terms in each condition. Once enriched GO terms aggregated at the same GO tree level, one Biological Process term can be encompassed under multiple higher GO terms. Thus, the number of enriched GO terms do not correspond to the number of Biological Process involved in each condition. These Biological Processes and the associated DEG expression levels are displayed in Figure 3. The response of diatoms exposed to $FLG_{50}$ involved the highest number of Biological Processes (14) when compared to FLG shading condition (12) and low FLG concentration (6). The rest of the functional analysis, based on DEGs description, focused only on DEGs associated to enriched GO terms.

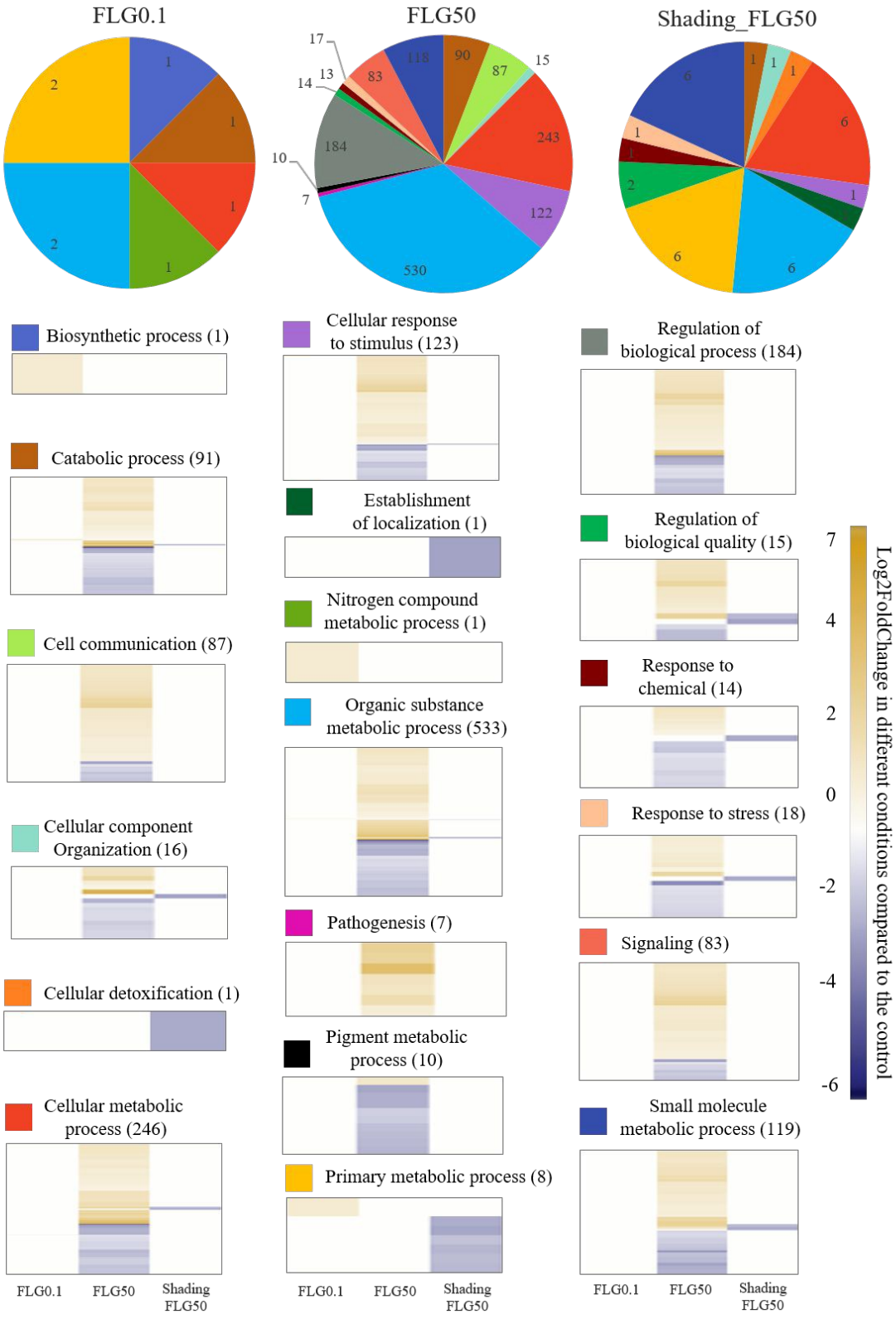


***Figure 3.*** *Biological processes involved and regulation of gene expression in the three different conditions. Pie charts present the distribution of GO terms associated with the DEGs relative to the control condition. Heat maps show profiles of gene expression for each biological process represented in pie charts. Numbers in pie charts and heat maps indicated the number of DEGs contributing to biological process.*

#### 3.4.1. Diatoms exposed to low FLG concentration

Results of GO enrichment revealed that only two slightly up-regulated DEGs (Log2FC values of 1.1±0.3 and 1.2±0.3) were associated with enriched GO terms for diatoms exposed to low FLG concentration. The first DEG (TT00_diatome_k49_Locus_3452_Transcript_7_1) might encoded for a platelet activating factor acetylhydrolase-like protein (PAF-AH, e-value = 7.7E-33) which is involved in the deacetylation of the PAF protein leading to a loss of activity but can also protect cells from oxidative stress by suppressing oxidized phospholipids[59]. The other DEG (TG01_diatome_k49_Locus_9856_Transcript_3_1) could correspond to a proline rich protein (PRP, e-value = 4.5E-5), a protein region observed in the frustulin, associated with the silica-based substructure of the diatom cell wall (frustule)[60,61]. Low FLG concentration elicited a slight transcriptomic response in diatoms and didn't result in cellular damages, in accordance with the absence of toxic effects evidenced in a previous study[24].

#### 3.4.2. Diatoms exposed to high FLG concentration

In the direct $FLG_{50}$ exposure, it was previously shown that after 48h diatoms presented cellular toxicity signs, as revealed by a growth rate inhibition and a loss of cell viability[24]. In the present study, 31.4% of the total DEGs presented a GO term and a BLAST homology (Table S1). The contribution to biological processes and Log2FC values of each discussed DEG is shown in the Table S2.

##### 3.4.2.1. DNA alteration and transcription machinery modifications

One of the 10 most down-regulated DEGs (OG50_diatome_k43_Locus_923_Transcript_10_2) participating to these biological processes could encode for a DNA helicase homologue. The down-regulation of this enzyme involved in several crucial cellular processes such as DNA replication and transcription[62] suggested a genomic regulation in response to a stimulus. DNA helicases are also known to be the first agent encountering DNA damages, and then can be highly involved in the DNA repair after mutations due to chemical expositions or radiations[63]. As this transcript is down-regulated in our study, exposure to high FLG concentration did not seemed to generate genetic damages in the diatom *N. palea*.

Several DEGs among the 10 most up-regulated ones presented GO terms related with DNA modification. One of these DEGs (TG01_diatome_k25_Locus_4662_Transcript_10_1) was described as a Rho termination factor with specific mRNA binding site. Rho termination

factor acts as an helicase to disengage mRNA from DNA and RNA polymerase[64]. This transcription factor was primarily discovered in *Escherichia coli* and known to be present in bacteria[65]. A Rho termination factor-like protein was also identified in higher plants plastids[66]. Interestingly, regulatory mechanisms associated with Rho termination factors have not been described yet in diatoms[67].

#### 3.4.2.2. Impact on post-translational modifications

Moreover, two major up-regulated DEGs, a SPT2 homolog (TG01_diatome_k37_Locus_4954_Transcript_4_1), which is a chromatin component, and a winged helix DNA-binding domain-containing protein (TG01_diatome_k49_Locus_8534_Transcript_3_1) participated to the regulation of biological process (9.6% of the 1907 DEGs expressed in this condition) and cellular component organization (1.31%). These putative proteins play a role in the transcription and post-transcriptional regulations[68]. In the 10 most down-regulated DEGs, the presence of three DEGs participating to the organic substance metabolic process, suggested a decrease in post-translational protein modification process with a down-regulation of peptidyl-prolyl cis-trans isomerase (OG50_diatome_k49_Locus_999_Transcript_1_1), calcium calmodulin dependent kinase association-domain protein (TT00_diatome_CL2065Contig1_2) and peptidase S8 (TG01_diatome_k49_Locus_13094_Transcript_1_1). These results might suggest that cells established regulation processes in response to the stress generated by the presence of high FLG concentration. This response is likely to be linked with the growth recovery previously observed[24] after a temporary growth inhibition at 48h of $FLG_{50}$ exposure. Diatoms were then able to implement an efficient response to reduce toxic effects induced by $FLG_{50}$ exposure which is in accordance with the modification of regulation processes observed in this work.

### 3.4.2.3. Cell wall alterations and cell adhesion system

Two up-regulated DEGs, participating to these biological processes, presented the same protein identification referring to a vegetative cell wall gp1-like (TT00_diatome_k25_Locus_575_Transcript_22_1; TG01_diatome_k49_Locus_14252_Transcript_2_1) that is a glycoprotein described as a major component of the outer cell wall layer of the green microalgae *Chlamydomonas reinhardtii*[69]. In a previous study evaluating the cell viability by fluorescent marking, toxicity effect induced by $FLG_{50}$ exposure was assumed to partly result from cellular wounds generated by the physical contact between cells and FLG nanoparticles[24]. Indeed, in some diatoms from the population exposed to $FLG_{50}$, wounds and cell wall distortions were evidenced by scanning electron microscopy (Figure 4b-d). The physical interaction could

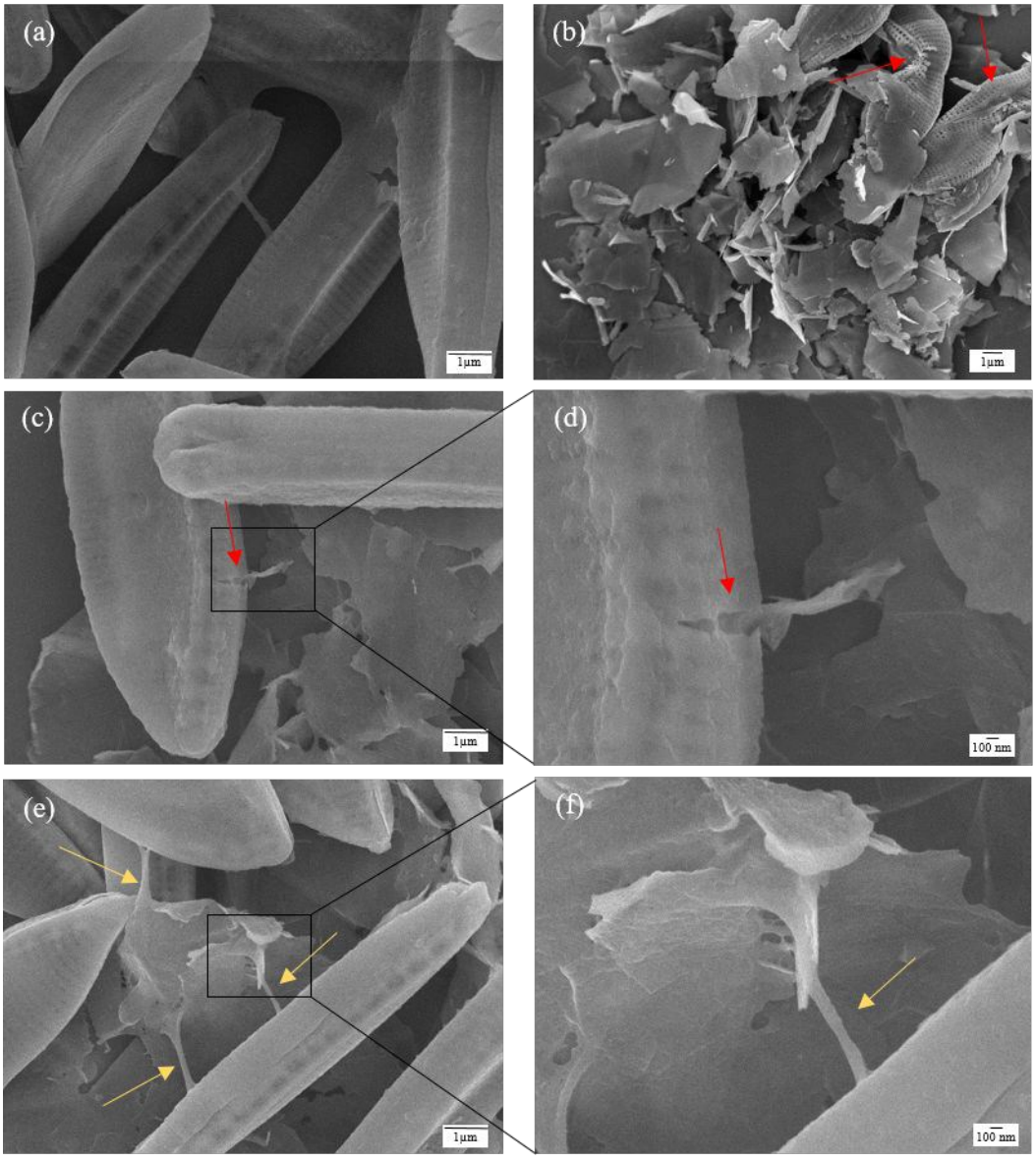


***Figure 4****. Scanning electron microscopy images of* N. palea *at 48 h of growth in control culture (a) and in culture exposed to $FLG_{50}$ (b-f). Red arrows indicate a wound or distortion of the cell wall and yellow ones indicate EPS matrix.*

partly explain the alteration of the global metabolism, as observed by Pohnert (2000)[70] who found that the diatoms *Thalassiosira rotula* and *Asterionella formosa* overproduced $C_{20}$ fatty acids in response to mechanical cell damages, reproducing herbivorous impact, as a chemical defence by high local concentration of defensive metabolites. The upregulation of the transcript encoding this protein suggests a potential cell wall repair as a consequence of wounds induced by physical contact with $FLG_{50}$.

The analysis of transcripts annotated with a Cellular Component category of Gene Ontology revealed an interesting result. Indeed, 50 DEGs belonged to extracellular region and membrane, with a majority of up-regulated transcripts (76%). Notably, the DEG with the highest overexpression might encode for a protein located in the extracellular matrix (TT00_diatome_CL78Contig1_1, see Table 1). Among the extracellular proteins, adhesin protein (OG50_diatome_CL14Contig2_1), non-classical arabinogalactan 31 (AGP31) (TG01_diatome_k49_Locus_7415_Transcript_3_1), a lpxtg-motif cell wall anchor domain protein (OG50_diatome_CL37Contig1_3) and a filamentous hemagglutinin family N-terminal domain protein (OG50_diatome_CL11Contig3_2) were highly up-regulated (Log2FC = 5). AGP31 was found to be a proteoglycan that may contribute to the strengthening of cell walls in *Arabidopsis thaliana*[71]. Willis *et al*. (2014)[72] also hypothesized that a protein sharing weak similarities with AGP31 (PDC4) was involved in the adhesion of *P. tricornutum* directly on substrate. A protein homologous to a filamentous hemagglutinin domain was described as a bacterial adhesin, especially for the bacteria *Bordetella pertussis*, allowing for cellular adhesion[73]. Our results suggest that the excretion of proteins involved in adhesion process was highly activated in the $FLG_{50}$ direct exposure (Figure 4e-f).

Biofilm formation, by keeping cells close to each other, promote strong cells interactions including cell-cell communication and the formation of synergistic microconsortia[21]. After the detection of environmental stress, marine diatoms cells are able to modulate infochemicals synthesis, such as nitric oxide, to induce cell-cell communication but also biofilm formation[74]. Thus, cell communication and adhesion process thanks to the EPS external production can both be consequences of environmental stress. Several molecular components of the extracellular matrix can be involved in the *N. palea* response to $FLG_{50}$ exposure, such as polysaccharides (in our dataset 9 chitin-binding protein were overexpressed in this condition), which are known to represent a non-negligible part of the EPS matrix[75], and specific protein (adhesin and AGP31 for instance)[72]. The induction of adhesive protein excretion as a response to the presence of high FLG concentration is consistent with previous nanotoxicological

studies. Verneuil *et al*., (2015)[23] demonstrated an EPS overproduction and excretion, especially the protein part of them, by *N. palea* exposed to carbon nanotubes. This is also supported by the observation of FLG sticking in the external matrix, which was already pointed as a mitigation to FLG toxicity[24]. Although EPS overproduction is a well-known mechanism occurring in a wide range of microorganisms exposed to many types of contaminants[76–78], little is known about the structure, mechanisms and specificity of these over-produced EPS. Our study provided valuable insights into the biochemical characteristics of the EPS over-excreted by *N. palea* exposed to FLG. This defence mechanism may lead to a modification of biofilm composition with more extracellular matrix and less cells.

#### 3.4.2.4. Photosynthetic activity and redox process

One upregulated DEG probably encoded for a phosphoribosylamine-glycine ligase (Log2FC = 1.4). Among the most downregulated DEGs, 16 participated in the pigment biosynthetic pathway, encoding for 10 enzymes or proteins complexes (Table S3). The position of enzymes encoded by these transcripts in the pigment biosynthetic pathway are represented in the Figure 5. Among these DEGs, an Aminolevulinate (ALA) dehydratase started this metabolic pathway in the cytoplasm forming porphobilinogen, the first pyrrole. Moreover, an uroporphyrinogen III synthase and three uroporphyrinogen decarboxylase were found as potential products of DEGs being part of the most down-regulated transcripts. These tetrapyrroles enzymes are involved in the porphyrin biosynthesis which enter in the chlorophyll biosynthesis and then play a role in the photosynthesis process[79]. Enzymes catalysing reactions of the rest of the metabolic pathway, such as protoporphyrinogen IX oxidase, ferrochelatase, protoporphyrin IX methyltransferase, geranyl reductase and chlorphyll synthetase were all found in down-regulated DEGs. Two DEGs described as light harvesting complex and two others encoding for fucoxanthin chlorophyll a c binding protein were also included in this down-regulated DEGs group. Taken as a whole, the under-expression of these 17 transcripts suggest a reduction of photosynthesis as a result of exposure to $FLG_{50}$. An hypothesis could be ventured to which genes encoding for enzymes involved in this pathway could be located in the plastid genome and then could be regulated by the Rho termination factor which is nuclear-encoded (for detailed discussion see Appendix 2) A reduction of photosynthetic activity thanks to photosystem II quantum yield measurement was previously demonstrated for diatoms directly exposed to $FLG_{50}$ [24], which is in full agreement with the transcriptomic response identified here.

Besides, DEGs encoding for a glutathione S-transferase and a glutaredoxin (OG50_diatome_k43_Locus_7159_Transcript_3_1;TG01_diatome_k49_Locus_5581_Transcript_1_1, Log2FC = -2.7; -2.6, respectively) were part of the most down-regulated transcripts. These proteins are known to act against oxidative stress by maintaining redox homeostasis[80], as demonstrated by Poirier and co-workers (2018)[81] studying *P. tricornutum* exposed to cadmium selenide nanocrystals. The down-regulation of these transcripts in our case suggests that $FLG_{50}$ exposure might be associated with a lower oxidative condition than in control. The down-regulation of oxidative stress management could be linked to the reduction of photosynthesis activity. Indeed, during photosynthesis, superoxide radicals production resulting in electron transfer from PS-I to oxygen is one of the major source of ROS generation in plants leading to oxidative damages[82]. As a result of the marine diatom *P. tricornutum* acclimation to high light, Nymark and co-workers (2009)[83] revealed the up-regulation of gene encoding for enzymes involved in photosynthetic pigment biosynthesis and genes encoding specific proteins involved in ROS scavenging. This supports the relationship between light intensity exposure and ROS production. In the case of $FLG_{50}$ exposure, we can hypothesize the reverse regulation process, where lower photosynthetic activity leads to a decrease in ROS production, then genes associated with oxidative stress were downregulated in order to reduced ROS scavenging.

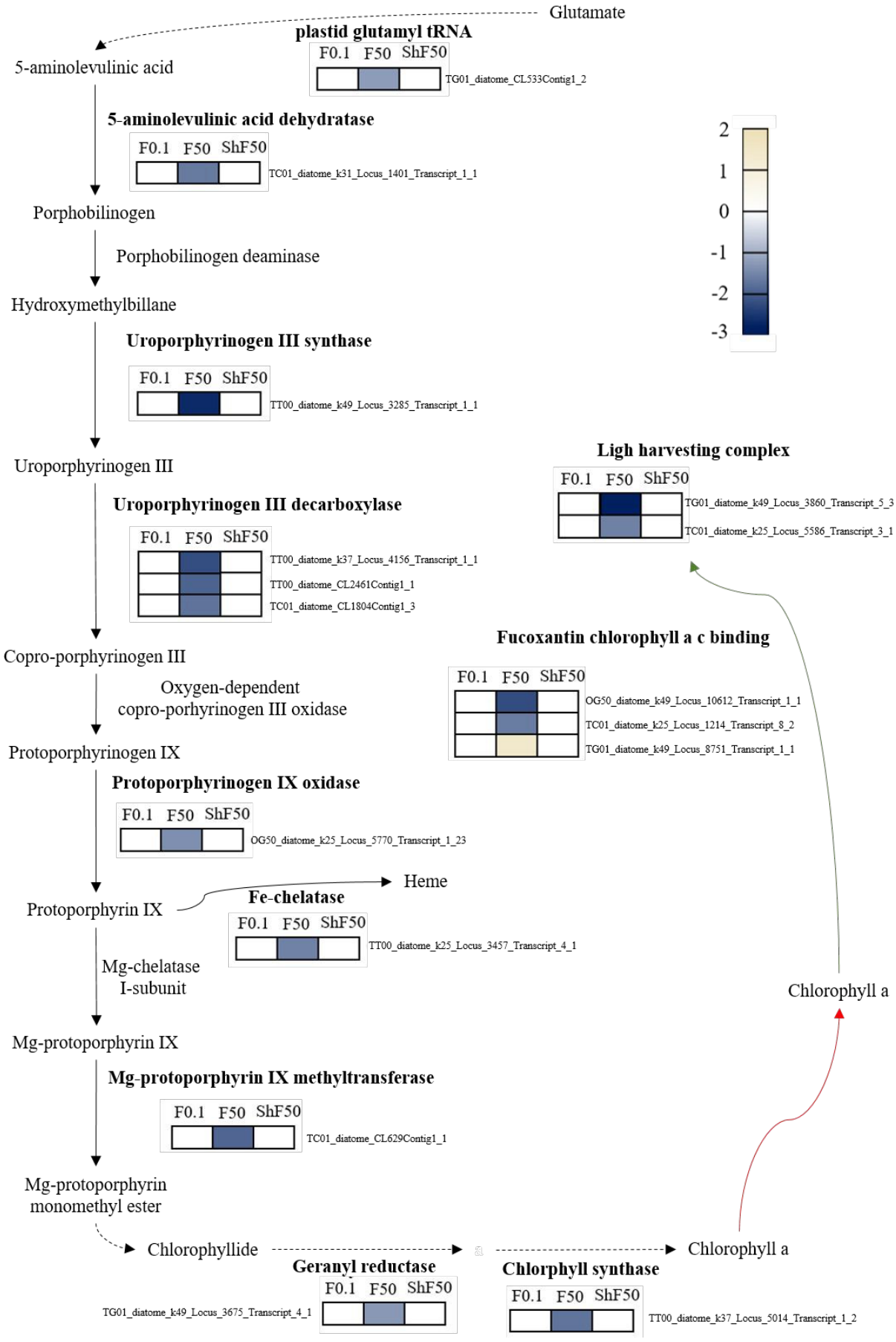
Glutamate
plastid glutamyl tRNA
F0.1 F50 ShF50
TG01_diatome_CL533Contig1_2
5-aminolevulinic acid
5-aminolevulinic acid dehydratase
F0.1 F50 ShF50
TC01_diatome_k31_Locus_1401_Transcript_1_1
Porphobilinogen
Porphobilinogen deaminase
Hydroxymethylbillane
Uroporphyrinogen III synthase
F0.1 F50 ShF50
TT00_diatome_k49_Locus_3285_Transcript_1_1
Uroporphyrinogen III
Uroporphyrinogen III decarboxylase
F0.1 F50 ShF50
TT00_diatome_k37_Locus_4156_Transcript_1_1
TT00_diatome_CL2461Contig1_1
TC01_diatome_CL1804Contig1_3
Copro-porphyrinogen III
Oxygen-dependent
copro-porhyrinogen III oxidase
Protoporphyrinogen IX
Protoporphyrinogen IX oxidase
F0.1 F50 ShF50
OG50_diatome_k25_Locus_5770_Transcript_1_23
Protoporphyrin IX
Heme
Fe-chelatase
F0.1 F50 ShF50
TT00_diatome_k25_Locus_3457_Transcript_4_1
Mg-chelatase
I-subunit
Mg-protoporphyrin IX
Mg-protoporphyrin IX methyltransferase
F0.1 F50 ShF50
TC01_diatome_CL629Contig1_1
Mg-protoporphyrin
monomethyl ester
Chlorophyllide
Geranyl reductase
F0.1 F50 ShF50
TG01_diatome_k49_Locus_3675_Transcript_4_1
Chlorophyll a
Chlorphyll synthase
F0.1 F50 ShF50
TT00_diatome_k37_Locus_5014_Transcript_1_2
2
1
0
-1
-2
-3
Ligh harvesting complex
F0.1 F50 ShF50
TG01_diatome_k49_Locus_3860_Transcript_5_3
TC01_diatome_k25_Locus_5586_Transcript_3_1
Fucoxantin chlorophyll a c binding
F0.1 F50 ShF50
OG50_diatome_k49_Locus_10612_Transcript_1_1
TC01_diatome_k25_Locus_1214_Transcript_8_2
TG01_diatome_k49_Locus_8751_Transcript_1_1
Chlorophyll a

***Figure 5***. *Chlorophyll a biosynthetic pathway in* N. palea *derived from Stenbaek and Jensen (2010)[68]. Coloured squares indicated the regulation of gene encoding for enzymes functioning (in bold) after 48h of exposure to $FLG_{0.1}$ (F0.1), $FLG_{50}$ (F50) and shading $FLG_{50}$ (ShF50). The scale on the right represents genes Log2FC value. Solid arrows indicate the conversion of each intermediate into the next and the involved enzymes are shown next one to each arrow. Dotted arrows indicate a reduction of chemical reaction to facilitate the reading of the figure. The red arrow indicates a transfer of chlorophyll a from cytoplasm to thylakoid membrane and the green arrow indicates a protein complex formation.*

These results suggest a global alteration of biological processes regulation to engage a response to contaminant, which can reveal an adaptive response to high FLG concentration. The impact on catabolic process could reveal a modification of the energy produced by cells. As evocated in previous works[24,40], diatoms could be able to induce energetic allocation from growth energy to EPS excretion pathway and response to stress in order to maintain a viable physiological level. Furthermore, the transcriptomic response suggesting an increase of extracellular proteins and polysaccharides production was only observed at high FLG concentration but not at low FLG concentration. The response between low and high FLG concentration was partly different and did not engage the same metabolic pathways. Slight transcriptomic response with low impact on the diatoms physiology was induced in low FLG concentration, whereas a clear stress was detected in high FLG concentration with light harvesting decrease and a significant toxicity linked to a growth inhibition. Signs of cellular damages probably linked to physical interactions with nanoparticles could occur at low and high concentration but EPS overproduction was only induced when diatoms were exposed to $FLG_{50}$ where wounds were actually observed.

### 3.4.3. Diatoms exposed to FLG shading

GO enrichment of DEGs in response to $FLG_{50}$ shading resulted in 12 Biological Processes with 8 down-regulated DEGs associated. One single DEG (TG01_diatome_k31_Locus_5498_Transcript_4_1; Log2FC = -2.2) described as an ubiquitin super oxide dismutase. This protein is known to remove cellular superoxide radicals. The reduction of this mRNA expression suggested that cells response to oxidative stress was inhibited.

Functional description of the DEGs involved in diatoms' response to FLG shading revealed the down-regulation of one DEG encoding for a glyceraldehyde-3-phosphate dehydrogenase (GAPDH) (TC01_diatome_CL336Contig1_1), involved in glycolysis and gluconeogenesis processes. Enzymes involved in energetic metabolic pathways are represented in Figure 6 (Table S5 details the DEGs expression level and functional description). It was demonstrated

that in *Neurospora* this enzyme activity was not influenced by environmental stresses such as nitrogen deprivation, high temperature or osmotic stress, but it was controlled by circadian clock, closely linked to light availability[84]. Studies undertaken on *P. tricornutum* demonstrated that GAPDH was activated during dark period[85,86], which correspond to a period of time not exceeding 24h. Nevertheless, in the case of *N. palea* exposed to 48h of shading $FLG_{50}$, which is longer than a dark period, this enzyme was down-regulated. This observation suggests that the duration of light limited access induced a modification of carbon metabolic pathway. This metabolic adaptation could help to maintain a physiological homeostasis during light deprivation. This might be at the origin of cell growth rate decrease observed in a previous study[24].

In addition, three DEGs were respectively associated with a long-chain fatty acid protein with a CoA ligase activity (OG50_diatome_CL1759Contig1_2), an acyl-CoA dehydrogenase (TC01_diatome_k31_Locus_2434_Transcript_2_1), and a fatty acid oxidation alpha mitochondrial protein with a 3-hydroxyacyl-CoA dehydrogenase activity (OG50_diatome_k43_Locus_3019_Transcript_2_1). These three down-regulated DEGs were involved in the fatty acid beta-oxidation process which contribute to the production of energy from fatty acids, captured in the form of ATP. Another down-regulated DEG (TT00_diatome_k37_Locus_4335_Transcript_2_1) in this condition encoding for a 3-ketoacyl participated to several biological processes linked to the cellular organization and localization (establishment of localization and cellular component organization). The description and the MF of this putative protein, suggesting an acetyl-CoA C-acyltransferase activity, were in accordance with the activity of a 3-ketoacyl-CoA thiolase, also involved in the fatty acid beta oxidation process. Thus we can hypothesize that the 3-ketoacyl protein described in our dataset is a 3-ketoacyl-CoA thiolase. This catabolic pathway provides the major source of energy for ATP production[87], but to start the oxidation process, fatty acids must be activated by acyl CoA synthase to form acyl-CoA, which consumes ATP[88,89]. In the literature, the effect of environmental conditions, such as light intensity, nutrient availability and temperature, are known, for a long time, to influence the content and the composition of fatty acids in diatoms[90,91]. Exposition to high light intensity induced an accumulation of fatty acids in cells[90,91], but in the case of shading $FLG_{50}$ exposure, with limited access to light as previously demonstrated (Photosynthetic Active Radiation decrease)[24], the reverse phenomenon occurred and could result in a decrease of fatty acid oxidation.

Moreover, a DEG presumably corresponding to a homologous of isocitrate lyase (OG50_diatome_k37_Locus_300_Transcript_5_3) was down-regulated in this condition. This protein is known to be a part of the glyoxylate cycle, resulting in the formation of succinate, generally involved in carbon source deprivation[92], with ATP consumption[93]. This metabolic pathway is located in the peroxisome, where a part of oxidation reactions occur, as suggested by Kroth and co-workers (2008)[94]. The down-regulation of this enzyme could be linked to the inhibition of fatty acids beta oxidation that produces acetylCoA which is a substrate of the glyoxylate cycle. Another product of the glyoxylate cycle is the oxaloacetate (OAA) which is involved in numerous metabolic pathways such as fatty acids biosynthesis or gluconeogenesis process. A DEGs described as a gene encoding a phosphoenolpyruvate carboxykinase (PEPCK) (TT00_diatome_k37_Locus_2515_Transcript_3_1) was also down-regulated in shading $FLG_{50}$ condition. This enzyme, located in mitochondrion, catalyses the chemical reaction of OAA in phosphoenolpyruvate (PEP), which is a primary step to enter in the gluconeogenesis process and lipids production. No evidence of effect of light intensity on this enzyme activity was found in the literature but a study demonstrated the increase of transcripts associated with PEPCK during the induction of pH stress on a marine diatom[95]. This suggest that once exposed to certain environmental stresses, such as pH or salinity, the induction of PEPCK allowed cells to manage stress. However, in the case of shading $FLG_{50}$ exposure, the under-expression of PEPCK could mean that diatoms were not able to undertake efficient response to the stress generated. Glyoxylate cycle is generally involved in the glucose production from lipids such as fatty acids, thanks to the OAA obtained. And yet, decarboxylation of OAA by the PEPCK generating PEP was also inhibited in this condition. Our results highlighted that all these processes, needing energetic supply, were down-regulated suggesting a strong alteration of energetic metabolism of *N. palea* after 48h of shading $FLG_{50}$ exposure.

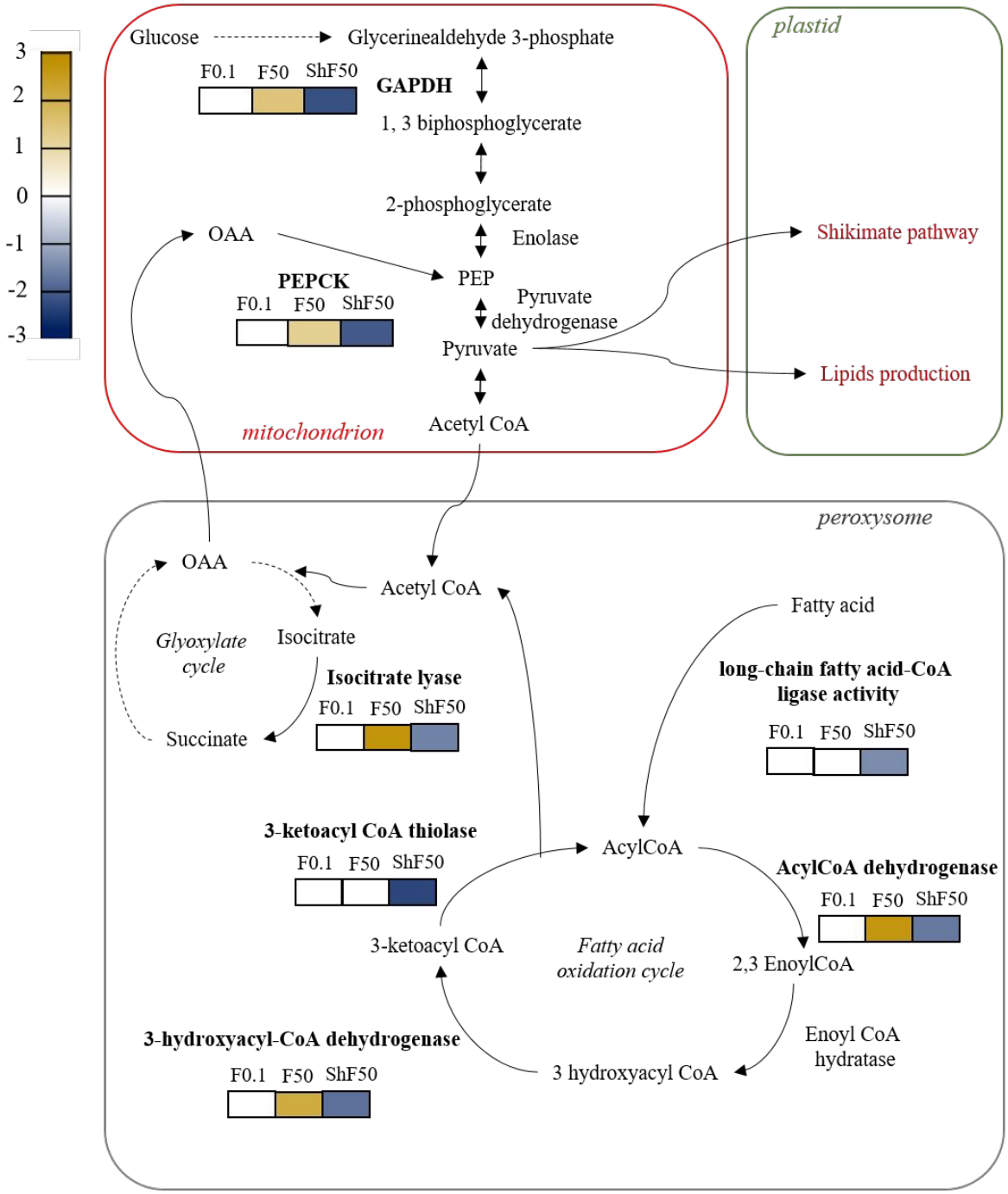


***Figure 6***. *Hypothesized energetic metabolic pathways in* N. palea*. Colored squares indicated the regulation of gene encoding for enzymes functioning (in bold) after 48h of exposure to FLG0.1 ($FLG_{0.1}$), FLG50 ($FLG_{50}$) and ShF50 (shading $FLG_{50}$). The scale on the left represents genes Log2FC value. Solid arrows indicate the conversion of each intermediate into the next one and the involved enzymes are shown next to each arrow. Dotted arrows indicate a reduction of chemical reaction to facilitate the reading of the figure. For simplicity, the number of organelle membranes has been reduced in this figure. This schematic view was adapted from Kroth and co-workers (2008)[94] and Heydarizadeh et al., (2014)[96].*

$FLG_{50}$ shading seemed to more generally inhibit the energetic metabolism of diatoms despite the slight number of DEGs involved. The reduction of basic metabolism might evidence an energetic preservation waiting for optimal environmental conditions for proliferation. Interestingly, this downregulation mechanism was effective after 48h of $FLG_{50}$ shading

exposure whereas it was undetected or even opposite after 48h of $FLG_{50}$ direct exposure (Figure 6). This phenomenon could be explained by the fact that under shading condition, cells response could not have an effective feedback on the shading stress. Indeed, in that case, cells were not in contact with nanoparticles and that sticking of $FLG_{50}$ in the extracellular matrix was not possible. An hypothesis could be that the down regulation mechanisms reported with $FLG_{50}$ shading might have occurred at the very beginning of the $FLG_{50}$ direct exposure, followed by a recovery of basal expression after FLG sticking associated with a clarification of the culture medium (i.e. mitigation of shading effect) before 48h[24].

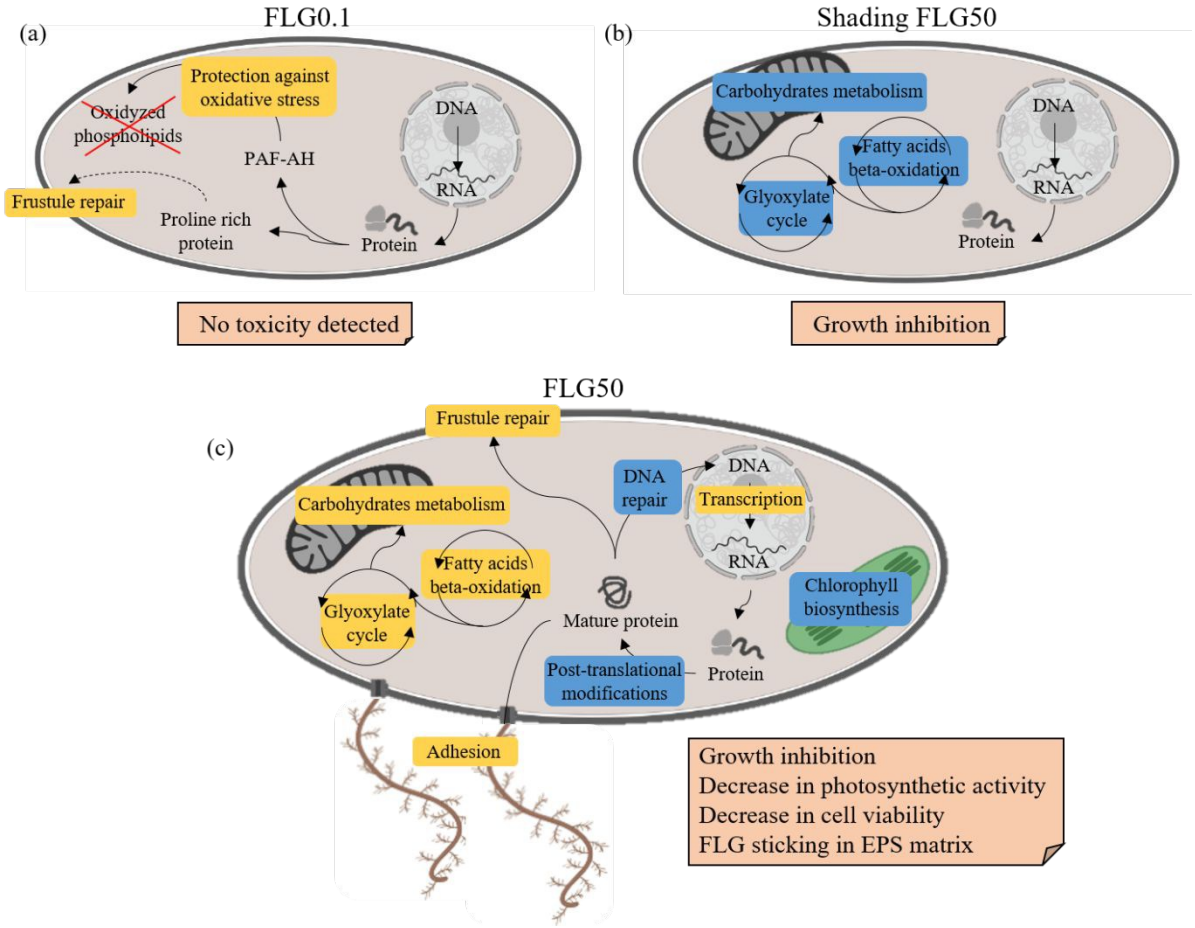


***Figure 7.****Adaptative pathways of* N. palea *in the response to direct FLG exposure at low ($FLG_{0.1}$)(a) and high ($FLG_{50}$)(c) concentration, and in shading exposure (Shading $FLG_{50}$) (b). Biological processes appearing in yellow were up-regulated and the ones appearing in blue were down-regulated. The transcriptomic response is compared to the cellular toxicity at 48h of FLG exposure assessed in* Garacci et al. (2017)[24] *indicated in the boxes.*

The stress induced in the shading and the direct $FLG_{50}$ exposure was absolutely not the same despite the presence of shared DEGs. A majority of these was up-regulated in direct exposure while they were all down-regulated in the shading exposure. The low percentage of similar DEGs regulated in the same way was mostly lost after the GO enrichment analysis. Contrary

to the shading exposure, the direct contact of $FLG_{50}$ mostly up-regulated the transcription of DEGs involved in the fatty acids oxidation. Diatoms exposed to shading and direct FLG exposure exhibited a specific response to the stress caused by direct contact or shading, which could help to adapt their physiological functions. Production of extracellular proteins involved in the direct exposure was not found in the shading effect suggesting that the contact and/or the toxicity induced by direct exposure was at the origin of this response. Hence, the two exposure modalities used in this study made it possible to disentangle the FLG effects due to contact or shading.

## 4. Conclusion

A transcriptomic approach was used to assess the effects of low and high FLG concentration in direct contact or in shading condition to identify the genes involved and the metabolic pathway affected in the different conditions. At low FLG concentration, close to anticipated environmental conditions, a slight transcriptomic response was induced in order to maintain the diatoms physiological state in accordance with the absence of growth inhibition. On the contrary, diatoms directly exposed to high FLG concentration exhibited a stronger transcriptomic response with differentially expressed genes involved in cell division and response to stress. No oxidative stress was identified but a decrease in photosynthetic metabolism gene expression was noticed suggesting a decrease in primary production. At the ecosystem level, this could eventually lead to a reduction in resources for grazers. An increase of transcripts encoding extracellular proteins with a role in the cellular adhesion confirmed previous results showing a sticking of FLG nanoparticles in the EPS matrix. The accumulation of FLG nanoparticles in the biofilm may then represent a risk of bioaccumulation for upper organisms. Few DEGs were shared between diatoms exposed to low and high FLG concentration, but the biological processes and the metabolic pathways mainly differed except for cellular division induction. In the shading condition, light deprivation induced a global slowing down of the metabolic activity of *N. palea*. This study highlighted that the number of DEGs expressed in a condition did not reflect the cellular response. In fact, a low number of DEGs were detected in diatoms exposed to low FLG concentration and shading, and yet a growth inhibition was only observed in the shading condition. In transcriptomic analysis, the function of DEGs must be prioritized over the number of DEGs.

Overall, this study gave insights into the specific biological processes and pathways involved in diatoms response to different FLG concentrations and exposition conditions. Nevertheless, transcriptomic study on the species *N. palea* present limits because the paucity of genomic and transcriptomic data available on diatoms impacted the annotation quality.

**Conflict of interest**

The authors report no conflict of interest.

**Acknowledgments**

This project has received funding from the European Union's Horizon 2020 research and innovation programme under grant agreement No 785219. Financial support for this study also was provided by the French Ministry of Higher Education and Research (PhD grant N°2015-73).

**References**


1 G. Brumfiel, .Consumer products leap aboard the nano bandwagon. *Nature*, 2006, 440, 262.

2 M. E. Vance, T. Kuiken, E. P. Vejerano, S. P. McGinnis, M. F. Hochella, D. Rejeski and M. S. Hull, .Nanotechnology in the real world: Redeveloping the nanomaterial consumer products inventory. *Beilstein J. Nanotechnol.*, 2015, **6**, 1769–1780.

3 M. J. Pitkethly, .Nanometerials - The driving force. *NanoToday*, 2004, **7**, 20–29.

4 X. Huang, Z. Yin, S. Wu, X. Qi, Q. He, Q. Zhang, Q. Yan, F. Boey and H. Zhang, .Graphene-based materials: Synthesis, characterization, properties, and applications. *Small*, 2011, **7**, 1876–1902.

5 C. Lee, X. Wei, J. W. Kysar and J. Hone, .Measurement of the elastic properties and intrinsic strength of monolayer graphene. *Science (80-. ).*, 2008, **321**, 385–388.

6 Y. Zhu, S. Murali, W. Cai, X. Li, J. W. Suk, J. R. Potts and R. S. Ruoff, .Graphene and graphene oxide: Synthesis, properties, and applications. *Adv. Mater.*, 2010, **22**, 3906–3924.

7 R. R. Nair, P. Blake, A. N. Grigorenko, K. S. Novoselov, T. J. Booth, T. Stauber, N. M. R. Peres and A. K. Geim, .Fine Structure Constant Defines visuals Transparency of Graphene. *Science (80-. ).*, 2008, **320**, 1308.

8 Z. Yan, D. L. Nika and A. A. Balandin, .Thermal properties of graphene and few-layer graphene: applications in electronics. *IET Circuits, Devices Syst.*, 2015, **9**, 4–12.

9 D. A. C. Brownson, D. K. Kampouris and C. E. Banks, .An overview of graphene in energy production and storage applications. *J. Power Sources*, 2011, **196**, 4873–4885.

10 X. Wang, L. Zhi and K. Müllen, .Transparent, conductive graphene electrodes for dye-sensitized solar cells. *Nano Lett.*, 2008, **8**, 323–327.

11 L. Feng and Z. Liu, .Graphene in biomedicine: opportunities and challenges. *Nanomedicine (Lond).*, 2011, **6**, 317–324.

12 F. Ahmed and D. F. Rodrigues, .Investigation of acute effects of graphene oxide on wastewater microbial community : A case study. *J. Hazard. Mater.*, 2013, **256**–**257**, 33–39.

13 D. R. Boverhof, C. M. Bramante, J. H. Butala, S. F. Clancy, W. M. Lafranconi, J. West and S. C. Gordon, .Comparative assessment of nanomaterial definitions and safety evaluation considerations. *Regul. Toxicol. Pharmacol.*, 2015, **73**, 137–150.

14 X. Hu and Q. Zhou, .Health and ecosystem risks of graphene. *Chem. Rev.*, 2013, **113**, 3815–3835.

15 A. Mottier, F. Mouchet, C. Laplanche, S. Cadarsi, L. Lagier, J. Arnault, H. A. Girard, V. Leon, E. Vazquez, C. Sarrieu, E. Pinelli, L. Gauthier and E. Flahaut, .Surface Area of Carbon Nanoparticles: A Dose Metric for a More Realistic Ecotoxicological Assessment. *Nano. Lett.*, 2016, **16**, 3514–3518.

16 A. Nel, T. Xia, L. Mädler and N. Li, .Toxic Potential of Materials at the Nanolevel. *Science (80-. ).*, 2006, **311**, 622–627.

17 A. Freixa, V. Acuña, J. Sanchís, M. Farré, D. Barceló and S. Sabater, .Ecotoxicological effects of carbon based nanomaterials in aquatic organisms. *Sci. Total Environ.*, 2018, **619–620**, 328–337.

18 M. S. Parker, T. Mock and E. V. Armbrust, .Genomic Insights into Marine Microalgae. *Annu. Rev. Genet.*, 2008, **42**, 619–645.

19 P. G. Falkowski, M. E. Katz, A. H. Knoll, A. Quigg, J. a Raven, O. Schofield and F. J. R. Taylor, .The Evolution of Modern Eukaryotic. *Science (80-. ).*, 2004, **305**, 354–360.

20 T. Watanabe, K. Asai and A. Houki, .Numerical estimation to organic pollution of flowing water by using the Epilithc Diatom Assemblge -Diatom Assemblage Index (DAIpo)-. *Sci. Total Environ.*, 1986, **55**, 209–218.

21 H. Flemming and J. Wingender, .The biofilm matrix. *Nature*, 2010, **8**, 623–633.

22 L. R. Andrade, R. N. Leal, M. Noseda, M. E. R. Duarte, M. S. Pereira, P. A. S. Mourão, M. Farina and G. M. Amado Filho, .Brown algae overproduce cell wall polysaccharides as a protection mechanism against the heavy metal toxicity. *Mar. Pollut. Bull.*, 2010, **60**, 1482–1488.

23 L. Verneuil, J. Silvestre, I. Randrianjatovo, C.-E. Maracato-romain, E. Girbal-Neuhauser, F. Mouchet, E. Flahaut, L. Gauthier and E. Pinelli, .Double walled carbon nanotubes promote the overproduction of extracellular protein-like polymers in Nitzschia palea : An adhesive response for an adaptive issue. *Carbon N. Y.*, 2015, **88**,

113–125.

24 M. Garacci, M. Barret, F. Mouchet, C. Sarrieu, P. Lonchambon, E. Flahaut, L. Gauthier, J. Silvestre and E. Pinelli, .Few Layer Graphene sticking by bio fi lm of freshwater diatom Nitzschia palea as a mitigation to its ecotoxicity. *Carbon N. Y.*, 2017, **113**, 139–150.

25 Q. Wang, S. Zhao, Y. Zhao and D. Wang, .Toxicity and translocation of graphene oxide in Arabidopsis plants under stress conditions. *RSC Adv.*, 2014, **4**, 60891–60901.

26 Q. Zhou and X. Hu, .Systemic Stress and Recovery Patterns of Rice Roots in Response to Graphene Oxide Nanosheets. *Environ. Sci. Technol.*, 2017, **51**, 2022–2030.

27 S. Deng, P.-P. Jia, J.-H. Zhang, M. Junaid, A. Niu, Y.-B. Ma, A. Fu and D.-S. Pei, .Transcriptomic response and perturbation of toxicity pathways in zebrafish larvae after exposure to graphene quantum dots (GQDs). *J. Hazard. Mater.*, 2018, **357**, 146–158.

28 M. Mortimer, N. Devarajan, D. Li and P. A. Holden, .Multiwall Carbon Nanotubes Induce More Pronounced Transcriptomic Responses in Pseudomonas aeruginosa PG201 than Graphene, Exfoliated Boron Nitride, or Carbon Black. *ACS Nano*, 2018, **12**, 2728–2740.

29 X. Hu, K. Lu, L. Mu, J. Kang and Q. Zhou, .Interactions between graphene oxide and plant cells: Regulation of cell morphology, uptake, organelle damage, oxidative effects and metabolic disorders. *Carbon N. Y.*, 2014, **80**, 665–676.

30 X. Hu, Y. Gao and Z. Fang, .Integrating metabolic analysis with biological endpoints provides insight into nanotoxicological mechanisms of graphene oxide: From effect onset to cessation. *Carbon N. Y.*, 2016, **109**, 65–73.

31 M. Lv, W. Huang, Z. Chen, H. Jiang, J. Chen, Y. Tian, Z. Zhang and F. Xu, .Metabolomics techniques for nanotoxicity investigations. *Bioanalysis*, 2015, **7**, 1527–1544.

32 T. H. Shin, D. Y. Lee, H. Lee, H. J. Park, M. S. Jin, M. Paik, B. Manavalan, J.-S. Mo and G. Lee, .Integration of metabolomics and transcriptomics in nanotoxicity studies. *BMB Rep.*, 2018, **51**, 14–20.

33 H. C. Poynton and C. D. Vulpe, .Ecotoxicogenomics: emerging technologies for emerging contaminants 1. *J. Am. Water Resour. Assoc.*, 2009, **45**, 83–96.

34 D. L. Villeneuve and N. Garcia-Reyero, .Vision & strategy: Predictive ecotoxicology in the 21st century. *Environ. Toxicol. Chem.*, 2011, **30**, 1–8.

35 Z. T. Muhseen, Q. Xiong, Z. Chen and F. Ge, .Proteomics studies on stress responses in diatoms. *Proteomics*, 2015, **15**, 3943–3953.

36 S. E. Hook, H. L. Osborn, F. Gissi, P. Moncuquet, N. A. Twine, M. R. Wilkins and M. S. Adams, .RNA-Seq analysis of the toxicant-induced transcriptome of the marine diatom, Ceratoneis closterium. *Mar. Genomics*, 2014, **16**, 45–53.

37 R. N. Carvalho, S. K. Bopp and T. Lettieri, .Transcriptomics responses in marine diatom Thalassiosira pseudonana exposed to the polycyclic aromatic hydrocarbon benzo[a]pyrene. *PLoS One*, 2011, **6**, e26985.

38 D. Nanjappa, R. Sanges, M. I. Ferrante and A. Zingone, .Diatom flagellar genes and their expression during sexual reproduction in Leptocylindrus danicus. *BMC Genomics*, 2017, **18**, 813.

39 M. M. N. Yung, P. Fougères, Y. H. Leung, F. Liu, A. B. Djurisic, J. P. Giesy and K. M. Y. Leung, .Physicochemical characteristics and toxicity of surface-modified zinc oxide nanoparticles to freshwater and marine microalgae. *Sci. Rep.*, 2017, **7**, 1–14.

40 L. Verneuil, J. Silvestre, F. Mouchet, E. Flahaut, J. Boutonnet, F. Bourdiol, T. Bortolamiol, D. Baqué, L. Gauthier and E. Pinelli, .Multi-walled carbon nanotubes , natural organic matter , and the benthic diatom Nitzschia palea : ‘“ A sticky story ”’. *Nanotoxicology*, 2014, **9**, 119–229.

41 M. Zheng, A. Jagota, E. D. Semke, B. A. Diner, R. S. McLean, S. R. Lustig, R. E. Richardson and N. G. Tassi, .DNA-assisted dispersion and separation of carbon nanotubes. *Nat. Mater.*, 2003, **2**, 338–342.

42 C. Cabau, F. Escudié, A. Djari, Y. Guiguen, J. Bobe and C. Klopp, .Compacting and correcting Trinity and Oases RNA-Seq de novo assemblies. *PeerJ*, , DOI:10.7717/peerj.2988.

43 B. J. Haas, A. Papanicolaou, M. Yassour, M. Grabherr, D. Philip, J. Bowden, M. B. Couger, D. Eccles, B. Li, M. D. Macmanes, M. Ott, J. Orvis, N. Pochet, F. Strozzi, N. Weeks, R. Westerman, T. William, C. N. Dewey, R. Henschel, R. D. LeDuc, N. Friedman and A. Regev, .De novo transcript sequence reconstruction from RNA-seq:

reference generation and analysis with Trinity. *Nat Protoc.*, 2013, **8**, 1–43.

44 B. Li and C. N. Dewey, .RSEM: Accurate transcript quantification from RNA-Seq data with or without a reference genome. *BMC Bioinformatics*, 2011, **12**, 1–16.

45 S. Götz, J. M. García-Gómez, J. Terol, T. D. Williams, S. H. Nagaraj, M. J. Nueda, M. Robles, M. Talón, J. Dopazo and A. Conesa, .High-throughput functional annotation and data mining with the Blast2GO suite. *Nucleic Acids Res.*, 2008, **36**, 3420–3435.

46 R Core Team, .R: a language and environment for statistical computing. *R Found. Stat. Comput. Vienna, Austria*.

47 M. I. Love, W. Huber and S. Anders, .Moderated estimation of fold change and dispersion for RNA-seq data with DESeq2. *Genome Biol.*, 2014, **15**, 1–21.

48 A. Alexa and J. Rahnenführer, .Gene set enrichment analysis with topGO. *Gene set enrichment analysis with topGO*, 2018.

49 D. Binns, E. C. Dimmer, R. P. Huntley, D. G. Barrell, D. Binns and R. Apweiler, .QuickGO: a web-based tool for Gene Ontology searching. *Bioinformatics*, 2009, **25**, 3045–3046.

50 G. R. Warnes, B. Bolker, L. Bonebakker, R. Gentleman, W. Huber and A. Liaw, .Various R programming tools for plotting data. *R Packag. version*, 2009, **2**, 1.

51 E. Neuwirth, .The RColorBrewer Package. *The RColorBrewer Package*, 2005.

52 H. Chen, .Generate High-Resolution Venn and Euler Plots. *Generate High-Resolution Venn and Euler Plots*, 2014.

53 E. J. Petersen, T. B. Henry, J. Zhao, R. I. MacCuspie, T. L. Kirschling, M. A. Dobrovolskaia, V. Hackley, B. Xing and J. C. White, .Identification and avoidance of potential artifacts and misinterpretations in nanomaterial ecotoxicity measurements. *Environ. Sci. Technol.*, 2014, **48**, 4226–4246.

54 E. V. Armbrust, J. A. Berges, C. Bowler, B. R. Green, D. Martinez, N. H. Putnam, S. Zhou, A. E. Allen, K. E. Apt, M. Bechner, M. A. Brzezinski, B. K. Chaal, A. Chiovitti, A. K. Davis, M. S. Demarest, J. C. Detter, T. Glavina, D. Goodstein, M. Z. Hadi, U. Hellsten, M. Hildebrand, B. D. Jenkins, W. W. Y. Lau, T. W. Lane, F. W. Larimer, J. C. Lippmeier, S. Lucas, A. Montsant, M. Obornik, M. S. Parker, B. Palenik, G. J.

Pazour, P. M. Richardson, T. A. Rynearson, M. A. Saito, D. C. Schwartz, K. Thamatrakoln, K. Valentin, A. Vardi, F. P. Wilkerson and D. S. Rokhsar, .The Genome of the Diatom. *Sciences (New. York).*, 2004, **306**, 79–87.

55 C. Bowler, A. E. Allen, J. H. Badger, J. Grimwood, K. Jabbari, A. Kuo, U. Maheswari, C. Martens, F. Maumus, R. P. Otillar, E. Rayko, A. Salamov, K. Vandepoele, B. Beszteri, A. Gruber, M. Heijde, M. Katinka, T. Mock, J. A. Berges, C. Brownlee, J. Cadoret, A. Chiovitti, K. Valentin, C. J. Choi, S. Coesel, A. De Martino, J. C. Detter, C. Durkin, A. Falciatore, P. J. Lopez, S. Lucas, E. Lindquist, M. Lommer, C. Napoli, M. Obornik, M. S. Parker, J. Petit and B. M. Porcel, .The Phaeodactylum genome reveals the evolutionary history of diatom genomes. *Nature*, 2008, **456**, 239–244.

56 M. Lommer, M. Specht, A. S. Roy, L. Kraemer, R. Andreson, M. A. Gutowska, J. Wolf, S. V. Bergner, M. B. Schilhabel, U. C. Klostermeier, R. G. Beiko, P. Rosenstiel, M. Hippler and J. LaRoche, .Genome and low-iron response of an oceanic diatom adapted to chronic iron limitation. *Genome Biol.*, , DOI:10.1186/gb-2012-13-7-r66.

57 T. Mock, R. P. Otillar, J. Strauss, M. McMullan, P. Paajanen, J. Schmutz, A. Salamov, R. Sanges, A. Toseland, B. J. Ward, A. E. Allen, C. L. Dupont, S. Frickenhaus, F. Maumus, A. Veluchamy, T. Wu, K. W. Barry, A. Falciatore, M. I. Ferrante, A. E. Fortunato, G. Glöckner, A. Gruber, R. Hipkin, M. G. Janech, P. G. Kroth, F. Leese, E. A. Lindquist, B. R. Lyon, J. Martin, C. Mayer, M. Parker, H. Quesneville, J. A. Raymond, C. Uhlig, R. E. Valas, K. U. Valentin, A. Z. Worden, E. V. Armbrust, M. D. Clark, C. Bowler, B. R. Green, V. Moulton, C. Van Oosterhout and I. V. Grigoriev, .Evolutionary genomics of the cold-Adapted diatom Fragilariopsis cylindrus. *Nature*, 2017, **541**, 536–540.

58 S. Moisset, S. K. Tiam, A. Feurtet-Mazel, S. Morin, F. Delmas, N. Mazzella and P. Gonzalez, .Genetic and physiological responses of three freshwater diatoms to realistic diuron exposures. *Environ. Sci. Pollut. Res.*, 2015, **22**, 4046–4055.

59 H. Arai, H. Koizumi, J. Aoki and K. Inoue, .Platelet-Activating Acetylhydrolase (PAF-AH). *J. Biochem.*, 2002, **131**, 635–640.

60 N. Kröger, C. Bergsdorf and M. Sumper, .Frustulins : domain conservation in a protein family associated with diatom cel walls. *Eur. J. Biochem.*, 1996, **239**, 259–264.

61 N. Kröger, G. Lehmann, R. Rachel and M. Sumper, .Characterization of a 200-kDa

diatom protein that is specifically associated with a silica-based substructure of the cell wall. *Eur. J. Biochem.*, 1997, **250**, 99–105.

62 S. W. Matson, D. W. Bean and J. W. George, .DNA Helicases: Enzymes with Essential Roles in All Aspects of DNA Metabolism. *BioEssays*, 1993, **16**, 13–22.

63 N. Tuteja, P. Ahmad, B. B. Panda and R. Tuteja, .Genotoxic stress in plants: Shedding light on DNA damage, repair and DNA repair helicases. *Mutat. Res. - Rev. Mutat. Res.*, 2009, **681**, 134–149.

64 D. L. Kaplan and M. O'Donnell, .Rho factor: Transcription termination in four steps. *Curr. Biol.*, 2003, **13**, 714–716.

65 A. Das, D. O. N. Court and S. Adhya, .Isolation and characterization of conditional lethal mutants of Escherichia coli defective in transcription termination factor rho. *Proc. Natl. Acad. Sci.*, 1976, **73**, 1959–1963.

66 W. Chi, B. He, N. Manavski, J. Mao, D. Ji, C. Lu, J. D. Rochaix, J. Meurer and L. Zhang, .RHON1 Mediates a Rho-Like Activity for Transcription Termination in Plastids of Arabidopsis thaliana. *Plant Cell*, , DOI:10.1105/tpc.114.132118.

67 A. Montsant, A. E. Allen, S. Coesel, A. De Martino, A. Falciatore, M. Mangogna, M. Siaut, M. Heijde, K. Jabbari, U. Maheswari, E. Rayko, A. Vardi, K. E. Apt, J. A. Berges, A. Chiovitti, A. K. Davis, K. Thamatrakoln, M. Z. Hadi, T. W. Lane, J. C. Lippmeier, D. Martinez, M. S. Parker, G. J. Pazour, M. A. Saito and D. S. Rokhsar, .IDENTIFICATION AND COMPARATIVE GENOMIC ANALYSIS OF SIGNALING AND REGULATORY COMPONENTS IN THE DIATOM THALASSIOSIRA PSEUDONANA 1. 2007, **604**, 585–604.

68 P. Thebault, G. Boutin, W. Bhat, A. Rufiange, J. Martens and A. Nourani, .Transcription Regulation by the Noncoding RNA SRG1 Requires Spt2-Dependent Chromatin Deposition in the Wake of RNA Polymerase II. *Mol. Cell. Biol.*, 2011, **31**, 1288–1300.

69 P. J. Ferris, J. P. Woessner, S. Waffenschmidt, S. Kilz, J. Drees and U. W. Goodenough, .Glycosylated Polyrpoline II Rods with Kinks as a Structural Motif in Plant Hydroxyproline-Rice Glycoproteins. *Biochemistry*, 2001, **40**, 2978–2987.

70 G. Pohnert, .Wound-activated chemical defense in unicellular planktonic algae. *Angew.*

*Chemie - Int. Ed.*, 2000, **39**, 4352–4354.

71 M. Hijazi, D. Roujol, H. Nguyen-Kim, L. Del Rocio Cisneros Castillo, E. Saland, E. Jamet and C. Albenne, .Arabinogalactan protein 31 (AGP31), a putative network-forming protein in Arabidopsis thaliana cell walls? *Ann. Bot.*, 2014, **114**, 1087–1097.

72 A. Willis, M. Eason-Hubbard, O. Hodson, U. Maheswari, C. Bowler and R. Wetherbee, .Adhesion molecules from the diatom Phaeodactylum tricornutum (Bacillariophyceae): Genomic identification by amino-acid profiling and in vivo analysis. *J. Phycol.*, 2014, **50**, 837–849.

73 A. A. Weiss and E. L. Hewlett, .Virulence factors of bordetella pertussis. *Ann. Rev. Microbiol.*, 1986, **40**, 661–686.

74 A. Vardi, .Cell signaling in marine diatoms. *Commun. Integr. Biol.*, 2008, **1**, 134–136.

75 B. J. Bellinger, A. S. Abdullahi, M. R. Gretz and G. J. C. Underwood, .Biofilm polymers: Relationship between carbohydrate biopolymers from estuarine mudflats and unialgal cultures of benthic diatoms. *Aquat. Microb. Ecol.*, 2005, **38**, 169–180.

76 D. Davies, .Understanding biofilm resistance to antibacterial agents. *Nat. Rev. Drug Discov.*, 2003, **2**, 114–122.

77 A. Quigg, W. Chin, C. Chen, S.-J. Zhang, Y. Jiang, A. Miao, K. a Schwehr, C. Xu and P. H. Santschi, .Direct and Indirect Toxic Effects of Engineered Nanoparticles on Algae: Role of Natural Organic Matter. *Sustain. Chem. Eng.*, 2013, **1**, 686–702.

78 L. A. Luongo and X. Zhang, .Toxicity of carbon nanotubes to the activated sludge process. *J. Hazard. Mater.*, 2010, **178**, 356–362.

79 A. Stenbaek and P. E. Jensen, .Redox regulation of chlorophyll biosynthesis. *Phytochemistry*, 2010, **71**, 853–859.

80 M. D. Shelton, P. Boon Chock and J. J. Mieyal, .Glutaredoxin: Role in Reversible Protein S-Glutathionylation and Regulation of Redox Signal Transduction and Protein Translocation. *Antioxyd. Redox Signal.*, 2005, **7**, 348–367.

81 I. Poirier, M. Pallud, L. Kuhn, P. Hammann, A. Demortière, A. Jamali, J. Chicher, C. Caplat, R. K. Gallon and M. Bertrand, .Toxicological effects of CdSe nanocrystals on the marine diatom Phaeodactylum tricornutum: The first mass spectrometry-based

proteomic approach. *Ecotoxicol. Environ. Saf.*, 2018, **152**, 78–90.

82 P. Ahmad, M. Sarwat and S. Sharma, .Reactive oxygen species, antioxidants and signaling in plants. *J. Plant Biol.*, 2008, **51**, 167–173.

83 M. Nymark, K. C. Valle, T. Brembu, K. Hancke, P. Winge, K. Andresen, G. Johnsen and A. M. Bones, .An integrated analysis of molecular acclimation to high light in the marine diatom Phaeodactylum tricornutum. *PLoS One*, , DOI:10.1371/journal.pone.0007743.

84 M. L. Shinohara, J. J. Loros and J. C. Dunlap, .Glyceraldehyde-3-phosphate Dehydrogenase Is Regulated on a Daily Basis by the Circadian Clock. *J. Biol. Chem.*, 1998, **273**, 446–452.

85 M. Siaut, M. Heijde, M. Mangogna, A. Montsant, S. Coesel, A. Allen, A. Manfredonia, A. Falciatore and C. Bowler, .Molecular toolbox for studying diatom biology in Phaeodactylum tricornutum. *Gene*, 2007, **406**, 23–35.

86 A. E. Allen, J. LaRoche, U. Maheswari, M. Lommer, N. Schauer, P. J. Lopez, G. Finazzi, A. R. Fernie and C. Bowler, .Whole-cell response of the pennate diatom Phaeodactylum tricornutum to iron starvation. *Proc. Natl. Acad. Sci.*, 2008, **105**, 10438–10443.

87 H. Schulz, .Beta oxidation of fatty acids. *Biochim. Biophys. Acta*, 1991, **1081**, 109–120.

88 R. a Coleman, T. M. Lewin, C. G. Van Horn and M. R. Gonzalez-Baró, .Do long-chain acyl-CoA synthetases regulate fatty acid entry into synthetic versus degradative pathways? *J. Nutr.*, 2002, **132**, 2123–2126.

89 H. Suzuki, Y. Kawarabayasi, J. Kondo, T. Abe, K. Nishikawa, S. Kimura, T. Hashimoto and T. Yamamoto, .Structure and regulation of rat long-chain acyl-CoA synthetase. *J. Biol. Chem.*, 1990, **265**, 8681–8685.

90 S. H. Mortensen, K. Y. Børsheim, J. Rainuzzo and G. Knutsen, .Fatty acid and elemental composition of the marine diatom Chaetoceros gracilis Schütt. Effects of silicate deprivation, temperature and light intensity. *J. Exp. Mar. Bio. Ecol.*, 1988, **122**, 173–185.

91 P. G. Roessler, .Environmental Control of Glycerolipid Metabolism in Microalgae:

Commercial Implications and Future Research Directions. *J. Phycol.*, 1990, **26**, 393–399.

92 J. E. Cronan, Jr. and D. Laporte, .Tricarboxylic Acid Cycle and Glyoxylate Bypass. *EcoSal Plus*, , DOI:10.1128/ecosalplus.3.5.2.

93 H. L. Kornberg and N. B. Madsen, .The metabolism of $C_2$ compounds in micro-organisms. 3. Synthesis of malate from acetate via the glyoxylate cycle. *Biochem. J.*, 1958, **68**, 549–557.

94 P. G. Kroth, A. Chiovitti, A. Gruber, V. Martin-Jezequel, T. Mock, M. S. Parker, M. S. Stanley, A. Kaplan, L. Caron, T. Weber, U. Maheswari, E. V. Armbrust and C. Bowler, .A Model for Carbohydrate Metabolism in the Diatom Phaeodactylum tricornutum Deduced from Comparative Whole Genome Analysis. *PLoS One*, 2008, **3**, e1426.

95 F. Mus, J.-P. Toussaint, K. E. Cooksey, M. W. Fields, R. Gerlach, B. M. Peyton and R. P. Carlson, .Physiological and molecular analysis of carbon source supplementation and pH stress-induced lipid accumulation in the marine diatom Phaeodactylum tricornutum. *Appl. Microbiol. Biotechnol.*, 2013, **97**, 3625–3642.

96 P. Heydarizadeh, J. Marchand, B. Chenais, M. R. Sabzalian, M. Zahedi, B. Moreau and B. Schoefs, .Functional investigations in diatoms need more than a transcriptomic approach. *Diatom Res.*, 2014, **29**, 75–89.

# Table of contents entry

Few Layer Graphene induces strong physiological modifications as a survival strategy of *Nitzschia palea*, at cell and biofilm scale.